iScience

CellPress
OPEN ACCESS

Article

Activation of ductal progenitor-like cells from adult human pancreas requires extracellular matrix protein signaling

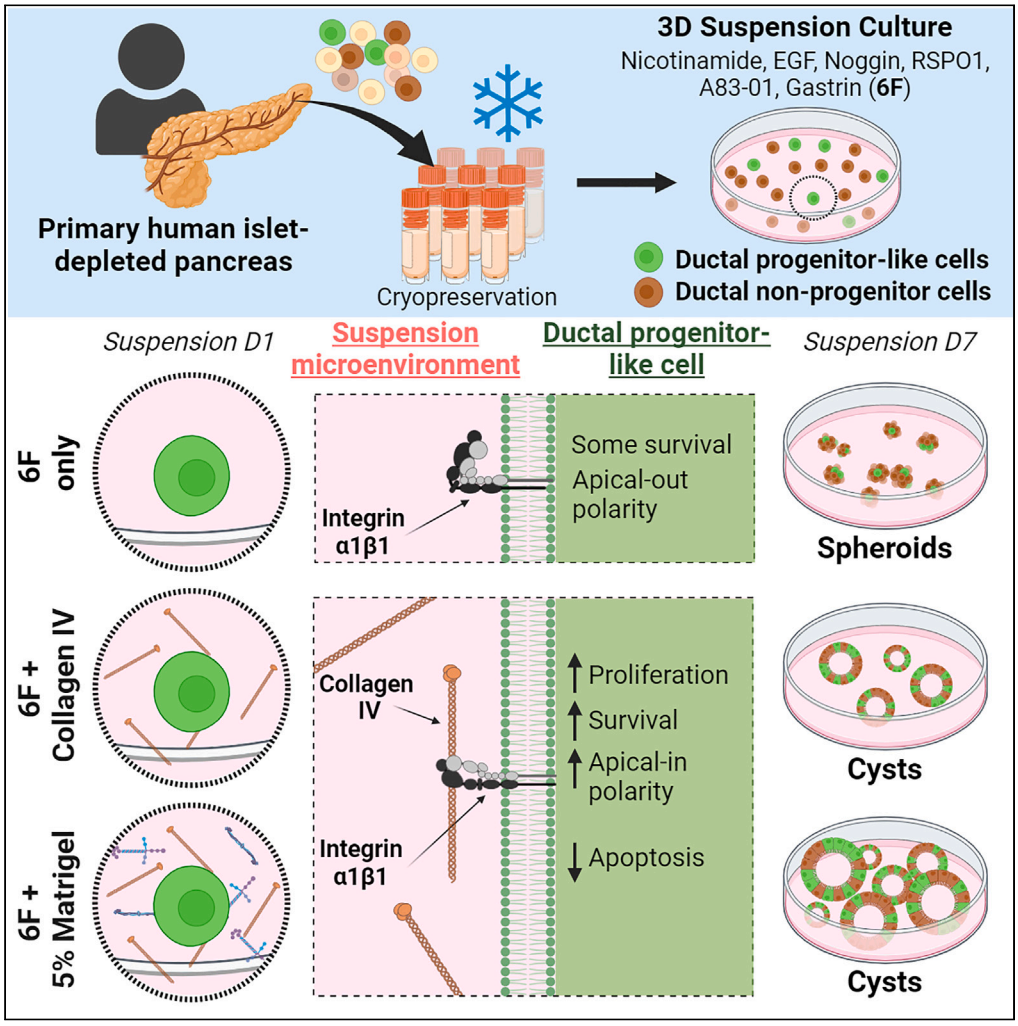

Heather N. Zook, Janine C. Quijano, Jose A. Ortiz, ..., Fouad Kandeel, Enrique Montero, Hsun Teresa Ku

hku@coh.org

Highlights

Human ductal, but not acinar, cells survive in a defined 3D suspension culture

Both ductal progenitor-like and ductal non-progenitor cells survive in culture

5% (v/v) Matrigel is sufficient to promote proliferation and apical-in polarity

Collagen IV partially recapitulates Matrigel's effects via integrin receptor α1β1

Zook et al., iScience 27, 109237
March 15, 2024
https://doi.org/10.1016/j.isci.2024.109237

iScience

CellPress
OPEN ACCESS

Article

Activation of ductal progenitor-like cells from adult human pancreas requires extracellular matrix protein signaling

Heather N. Zook,[1,2] Janine C. Quijano,[2] Jose A. Ortiz,[1,2] Cecile Donohue,[2] Kassandra Lopez,[2] Wendong Li,[2] Neslihan Erdem,[1,2,3] Kevin Jou,[2] Christiana J. Crook,[1,2,4] Isaac Garcia, Jr.,[3] Fouad Kandeel,[2] Enrique Montero,[3] and Hsun Teresa Ku[1,2,5,*]

SUMMARY

Ductal progenitor-like cells are a sub-population of ductal cells in the adult human pancreas that have the potential to contribute to regenerative medicine. However, the microenvironmental cues that regulate their activation are poorly understood. Here, we establish a 3-dimensional suspension culture system containing six defined soluble factors in which primary human ductal progenitor-like and ductal non-progenitor cells survive but do not proliferate. Expansion and polarization occur when suspension cells are provided with a low concentration (5% v/v) of Matrigel, a sarcoma cell product enriched in many extracellular matrix (ECM) proteins. Screening of ECM proteins identified that collagen IV can partially recapitulate the effects of Matrigel. Inhibition of integrin α1β1, a major collagen IV receptor, negates collagen IV- and Matrigel-stimulated effects. These results demonstrate that collagen IV is a key ECM protein that stimulates the expansion and polarization of human ductal progenitor-like and ductal non-progenitor cells via integrin α1β1 receptor signaling.

INTRODUCTION

The pancreas is composed of exocrine (including ductal and acinar cells) and endocrine compartments important for regulating food digestion and blood glucose levels, respectively. Death or dysfunction of pancreatic cells leads to diseases such as pancreatitis and diabetes, and repair of disease-driven injury by fully differentiated pancreatic cells is limited.[1,2]

In many organs, tissue-resident progenitor cells play important roles in maintaining homeostasis and regenerating cells after injury.[3,4] In the adult pancreas, it has been proposed that ductal cells can function as facultative progenitor cells and undergo proliferation in response to signals induced by pancreatitis or diabetes.[5–8] Recent reports indicate that a sub-population of adult human ductal cells displays progenitor-like properties.[9–12] However, the microenvironmental signals required for the survival, activation, and expansion of ductal progenitor-like cells remain largely unknown.

In recent years, primary human ductal cells have been successfully cultured using a 3-dimensional (3D) organoid culture system, which allows the identification and study of human ductal progenitor-like cells.[9,10] This organoid culture system uses high concentrations (>75% v/v) of Matrigel, which is derived from a murine sarcoma cell line enriched with extracellular matrix (ECM) proteins.[13] However, Matrigel is complex, varies from lot-to-lot, and its chemical and mechanical properties cannot be independently tuned,[14] precluding dissection of ECM protein-driven effects on ductal progenitor-like cells.

In this study, we aimed to elucidate microenvironmental signals required for the survival and activation of primary human ductal progenitor-like cells isolated from cadaveric donors without apparent disease. Here we report that: (1) a combination of six defined soluble factors is necessary for the survival, but not activation, of human pancreatic ductal progenitor-like and ductal non-progenitor cells in a 3D suspension culture, and (2) the ECM protein collagen IV is sufficient and necessary to initiate the activation of ductal progenitor-like and ductal non-progenitor cells via integrin α1β1 receptor signaling.

[1]Irell & Manella Graduate School of Biological Sciences, City of Hope National Medical Center, Duarte, CA 91010, USA
[2]Department of Translational Research and Cellular Therapeutics, Arthur Riggs Diabetes and Metabolism Research Institute, City of Hope National Medical Center, Duarte, CA 91010, USA
[3]Department of Diabetes Immunology, Arthur Riggs Diabetes and Metabolism Research Institute, City of Hope National Medical Center, Duarte, CA 91010, USA
[4]Present address: Department of Medical Oncology and Therapeutics Research, City of Hope National Medical Center, Duarte, CA 91010, USA
[5]Lead contact
*Correspondence: hku@coh.org
https://doi.org/10.1016/j.isci.2024.109237

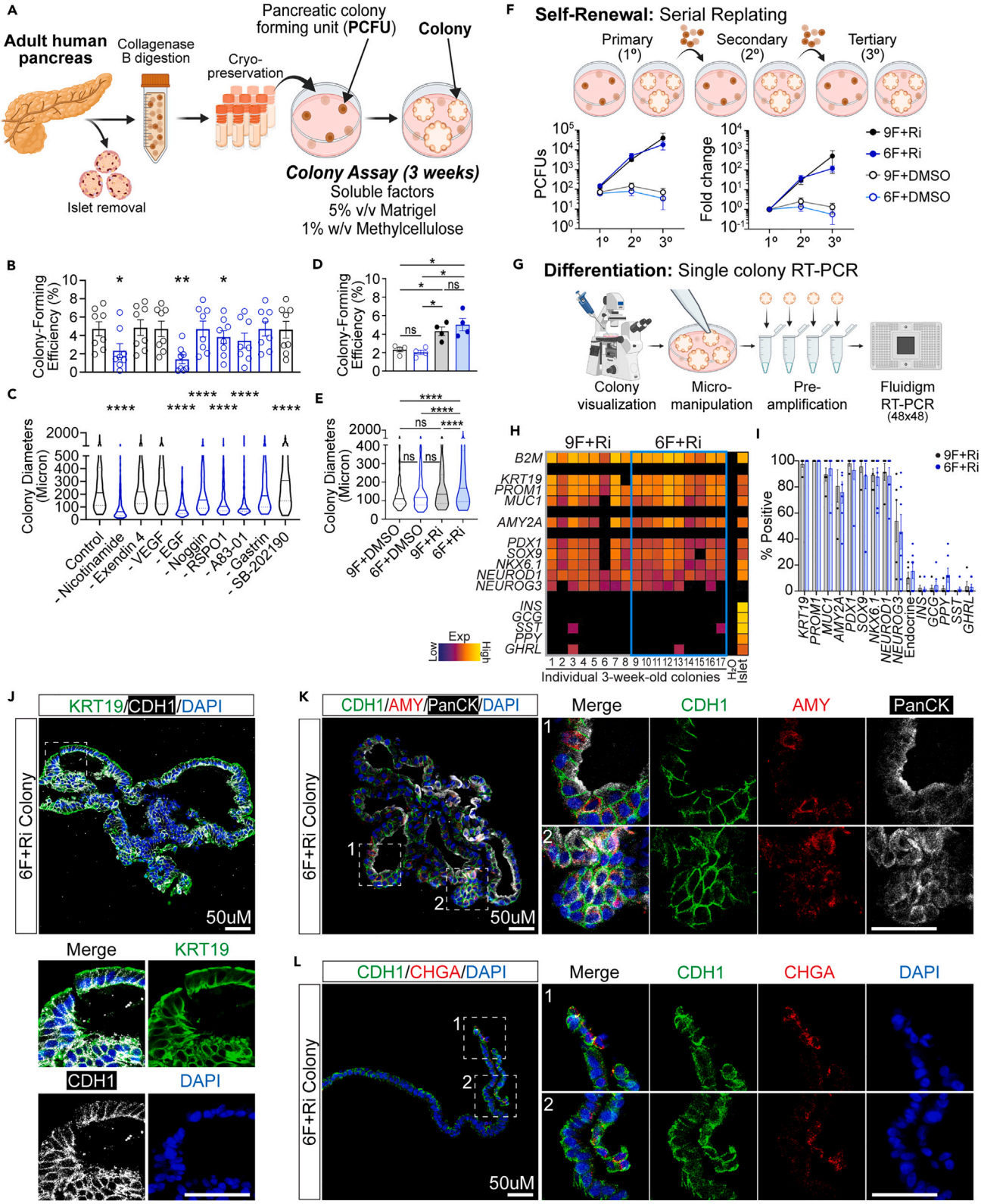
A
Adult human pancreas
Collagenase B digestion
Islet removal
Cryo-preservation
Pancreatic colony forming unit (PCFU)
Colony
Colony Assay (3 weeks)
Soluble factors
5% v/v Matrigel
1% w/v Methylcellulose
F
Self-Renewal: Serial Replating
Primary (1º)
Secondary (2º)
Tertiary (3º)
PCFUs
Fold change
9F+Ri
6F+Ri
9F+DMSO
6F+DMSO
B
Colony-Forming Efficiency (%)
D
Colony-Forming Efficiency (%)
C
Colony Diameters (Micron)
Control
- Nicotinamide
- Exendin 4
- VEGF
- EGF
- Noggin
- RSPO1
- A83-01
- Gastrin
- SB-202190
E
Colony Diameters (Micron)
9F+DMSO
6F+DMSO
9F+Ri
6F+Ri
G
Differentiation: Single colony RT-PCR
Colony visualization
Micro-manipulation
Pre-amplification
Fluidigm RT-PCR (48x48)
H
9F+Ri
6F+Ri
B2M
KRT19
PROM1
MUC1
AMY2A
PDX1
SOX9
NKX6.1
NEUROD1
NEUROG3
INS
GCG
SST
PPY
GHRL
Exp
Low
High
Individual 3-week-old colonies
H2O
Islet
I
% Positive
9F+Ri
6F+Ri
Endocrine
J
KRT19/CDH1/DAPI
6F+Ri Colony
50uM
Merge
KRT19
CDH1
DAPI
K
CDH1/AMY/PanCK/DAPI
6F+Ri Colony
50uM
Merge
CDH1
AMY
PanCK
L
CDH1/CHGA/DAPI
6F+Ri Colony
50uM
Merge
CDH1
CHGA
DAPI

Figure 1. Six soluble factors are sufficient to support survival and growth of human ductal progenitor-like cells in a methylcellulose colony assay

(A) Schematic for experimental design.

(B and C) Single-factor omission from nine factor (9F) colony assay medium. (B) Colony-forming efficiency quantification. Each dot is a donor. (C) Colony diameter measurements. Seeding density was 5,000 cells per well. N = 8 donors; (B) n = 4 technical replicates, (C) n = 20–50 individual colonies.

(D and E) Comparison of 9F and 6F media supplemented with Y-27632 (Ri, 10 μM) or vehicle (0.1% DMSO). (D) Colony-forming efficiency quantification. (E) Colony diameter measurements. Seeding density was 2,500 or 5,000 cells per well. N = 4 donors; (D) n = 4 technical replicates, (E) n = 20–50 individual colonies.

(F) Serial replating schematic and PCFU expansion quantification. N = 4 donors and n = 4 technical replicates.

(G) Schematic for single-colony micro-manipulation and microfluidic RT-PCR.

(H) Representative heatmap of microfluidic RT-PCR results from 3-week-old colonies cultured in 6F + Ri or 9F + Ri. Endocrine refers to individual colonies that expressed at least one of the endocrine genes (i.e., *INS*, *GCG*, *PPY*, *SST*, and *GHRL*).

(I) Percentage of 3-week-old colonies cultured in 6F + Ri or 9F + Ri that expressed selected genes. N = 6 donors, n = 8 individual colonies.

(J–L) Immunofluorescence (IF) staining of lineage markers in 3-week-old colonies cultured in 6F + Ri colony assay. Representative IF staining of: (J) Keratin 19 (KRT19; green) and MUCIN1 (MUC1; white); (K) E-cadherin (CDH1; green), Amylase (AMY; red), and pan-cytokeratin (PanCK; white); and (L) CDH1 (green) and chromogranin A (CHGA; red). DAPI was used to visualize nuclei in all colonies. N = 3 donors. Data are depicted as mean ± SEM (B, D, F, and I), or as violin plots (C and E). Statistical analysis used Student's *t* test comparing each test group against the control (B, paired; C, unpaired with Welch's correction) or one-way ANOVA with Tukey's correction (D, paired; E, unpaired), where *p < 0.05, **p < 0.01, ****p < 0.0001.

See also Figures S1 and S2.

RESULTS

Six soluble factors, compared to nine factors, are sufficient to support the survival and growth of human pancreatic ductal progenitor-like cells cultured in a methylcellulose colony assay

Primary and clinical-grade pancreatic exocrine tissues were obtained after isolation of islets (endocrine cells) from cadaveric human donors without apparent disease (Table S1) and were dissociated into a single-cell suspension before cryopreservation and/or experimentation. On average, the seventeen donors used in these studies were 29.0 ± 2.4 years of age, had a body mass index of 25.1 ± 1.0, and had a hemoglobin A1c of 5.1 ± 0.1%.

Previously, we established a methylcellulose-based colony assay for functional analyses (survival, differentiation, and self-renewal) of human ductal progenitor-like cells, which we named pancreatic colony-forming units (PCFUs)[12] (Figure 1A). Methylcellulose is a viscous, biologically inactive material[15] that prevents cellular aggregation and allows a single progenitor-like cell to form a colony in 3D space when appropriate factors are present. In addition to 1% (w/v) methylcellulose, our standard human colony assay contains 5% (v/v) Matrigel and nine defined recombinant growth factors and small molecules (9-factor, 9F): nicotinamide, epithelial growth factor (EGF), Noggin, exendin-4, SB202190, gastrin, R-spondin 1 (RSPO1), vascular endothelial growth factor (VEGF), and A83-01 (Table S2). However, it was unknown whether all nine factors were required. To test this, we performed single-factor omission experiments, in which each factor was removed from the 9F medium.

Colony-forming efficiency (percentage of 3-week-old colonies grown) and colony diameter serve as proxies for progenitor-like cell survival and proliferative capacity, respectively.[12,16,17] When nicotinamide, EGF, or RSPO1 was omitted, colony-forming efficiency decreased relative to the control 9F condition (Figure 1B), demonstrating the critical role of these factors for ductal PCFU survival. Omitting nicotinamide, EGF, Noggin, RSPO1, or A83-01 reduced colony diameters (Figure 1C), demonstrating that colony growth requires these factors. Among eight donors examined, two required the presence of gastrin for colony growth (Figure S1A). In contrast, colony diameters increased following omission of SB-202190 (Figure 1C), suggesting that SB-202190 is inhibitory to colony growth.

To determine whether exendin-4, VEGF, and SB-202190 are dispensable for our colony assay, six soluble factors—nicotinamide, EGF, Noggin, RSPO1, A83-01, and gastrin (6-factor, 6F)—were combined and their effects compared against 9F. We previously showed that Y-27632, a Rho-associated kinase (ROCK) inhibitor (Ri), improves PCFU survival and self-renewal in the 9F colony assay.[12] Therefore, we examined the effects of Ri on the 6F colony assay. Ri addition enhanced colony-forming efficiency by ~2-fold compared to the vehicle control (DMSO) regardless of whether 6F or 9F was included, confirming that PCFU survival is increased by Ri (Figure 1D). However, no difference was found between 6F and 9F (Figure 1D), suggesting equivalent support of PCFU survival. Consistent with the finding that omission of SB-202190 from 9F increased colony diameter (Figure 1C), 6F + Ri led to the largest colony diameters compared to all other conditions (Figure 1E). These results demonstrate that in the presence of Ri, 6F supports increased colony growth compared to 9F.

To further characterize the survival effect of Ri on PCFUs, we performed a delayed addition experiment in which Ri was added to 6F colony assay on days (D) 0 (positive control), 1, 2, 4, or 7. Addition of Ri on or after D1 reduced colony-forming efficiency compared to addition at D0, although colony-forming efficiency remained higher than that of vehicle control (6F + DMSO) (Figure S1B), demonstrating that Ri is critical for some PCFU survival on D0. Colony diameters were unaffected by the delayed addition of Ri except when Ri was added on D7 (Figure S1C), suggesting an unchanged proliferative potential of surviving PCFUs until D7 post-plating.

To determine whether self-renewal of PCFUs is affected by 6F + Ri compared to 9F + Ri, we performed serial dissociation and replating (Figure 1F).[12] Briefly, 3-week-old colonies grown in the primary colony assay were dissociated into single cells and then replated into a secondary colony assay. This was repeated once more for a tertiary colony assay, resulting in a 9-week expansion of PCFUs. Culture conditions without Ri did not support PCFU expansion, whereas the number of PCFUs supported over time by 6F + Ri was equivalent to 9F + Ri (Figure 1F), demonstrating that self-renewal was preserved in 6F + Ri condition.

The lineage potential of a PCFU is reflected in the lineages the PCFU gives rise to in a colony.[17,18] To determine whether lineage differentiation of PCFUs is affected by 6F + Ri compared to 9F + Ri, we micro-manipulated individual 3-week-old colonies and performed gene

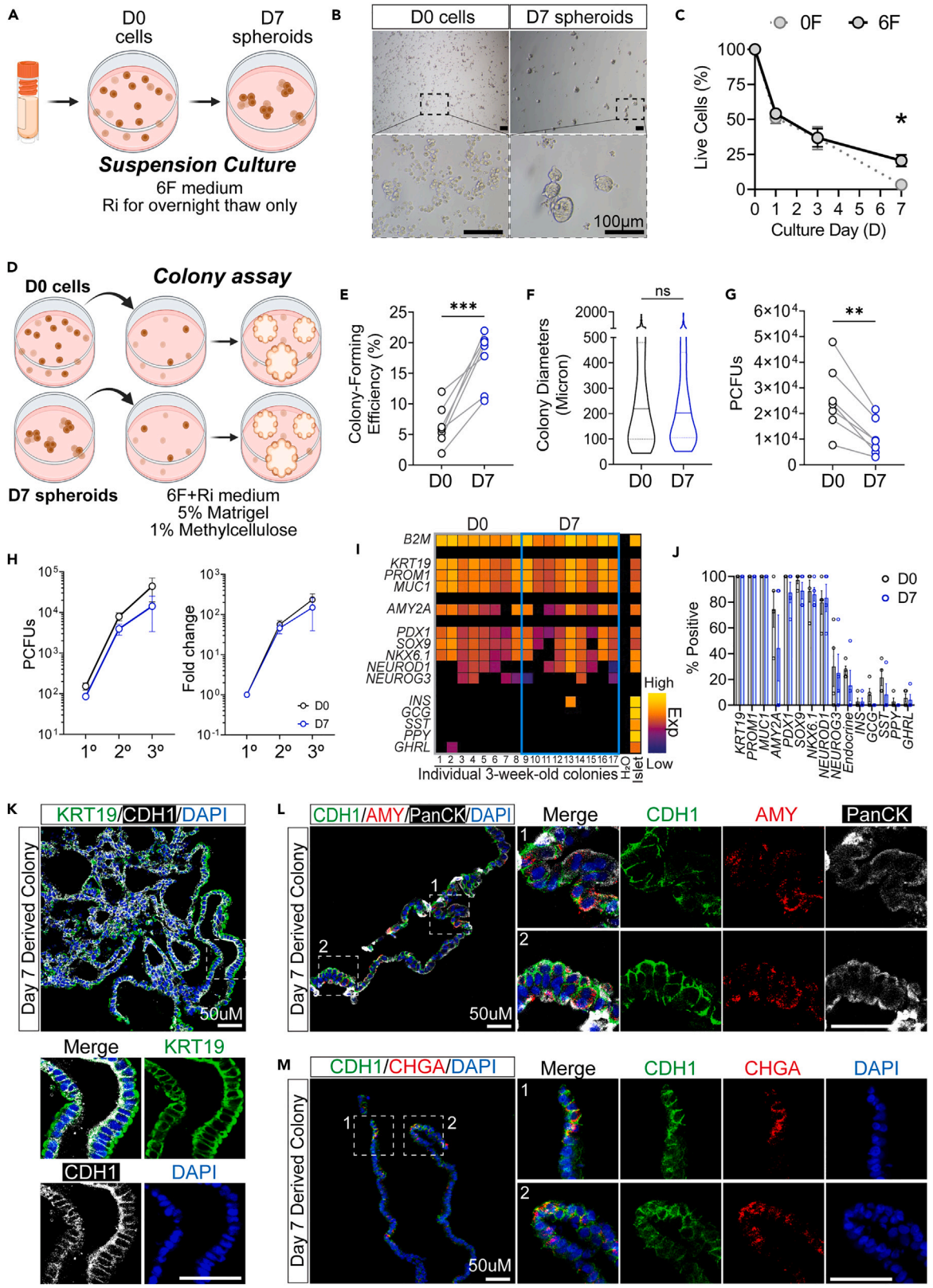
A
D0 cells
D7 spheroids
Suspension Culture
6F medium
Ri for overnight thaw only
B
D0 cells
D7 spheroids
100μm
C
0F
6F
Live Cells (%)
Culture Day (D)
*
D
D0 cells
Colony assay
D7 spheroids
6F+Ri medium
5% Matrigel
1% Methylcellulose
E
Colony-Forming Efficiency (%)
***
D0
D7
F
Colony Diameters (Micron)
ns
G
PCFUs
**
H
PCFUs
Fold change
D0
D7
I
B2M
KRT19
PROM1
MUC1
AMY2A
PDX1
SOX9
NKX6.1
NEUROD1
NEUROG3
INS
GCG
SST
PPY
GHRL
High
Exp
Low
Individual 3-week-old colonies
H2O
Islet
J
% Positive
Endocrine
K
KRT19/CDH1/DAPI
Day 7 Derived Colony
50uM
Merge
KRT19
CDH1
DAPI
L
CDH1/AMY/PanCK/DAPI
Merge
CDH1
AMY
PanCK
M
CDH1/CHGA/DAPI
Merge
CDH1
CHGA
DAPI

Figure 2. Six soluble factors are required for the survival of adult human pancreatic ductal progenitor-like cells in a 3D suspension culture

(A) 3D suspension culture schematic.

(B) Representative brightfield images at culture day (D)0 and D7. Scale bars: 100 μm.

(C) Percentage of live cells during suspension culture with or without 6F, relative to D0. N = 4 donors, n = 2 technical replicates.

(D) Schematic for cell replating into colony assay. D0 cells were plated at either 2,500 or 5,000 cells per well. D7 spheroids were dissociated and plated at either 500 or 1,000 cells per well. For each donor, both D0 and D7 cells were plated on the same day into the 6F + Ri colony assay.

(E–G) Comparison of D0 cells and D7 spheroids. (E) Colony-forming efficiency quantification. (F) Colony diameter measurements. (G) PCFU quantification, calculated by multiplying the colony-forming efficiency by the number of live cells per well at D0 or D7. Plating density was 500–5,000 cells per well. N = 7 donors; (E and G) n = 4 technical replicates, (F) n = 20–50 individual colonies.

(H) PCFU self-renewal quantification of D0 and D7 cells. N = 4 donors and n = 4 technical replicates.

(I and J) PCFU differentiation analysis. (I) Representative heatmap of microfluidic RT-PCR results and (J) percentage of colonies positive for selected genes from 3-week-old colonies derived from D0 or D7 cells. "Endocrine" refers to individual colonies that expressed at least one of the endocrine genes (i.e., *INS*, *GCG*, *PPY*, *SST*, and *GHRL*). N = 4 donors and n = 8–12 individual colonies.

(K–M) Immunofluorescence (IF) staining of lineage markers in 3-week-old colonies derived from dissociated D7 suspension cultured cells. Representative IF staining of: (K) KRT19 (green) and MUC1 (white); (L) CDH1 (green), AMY (red), and PanCK (white); and (M) CDH1 (green) and CHGA (red). DAPI was used to visualize nuclei in all colonies. N = 3 donors. Data are depicted as mean ± SEM (C, H, and J), donor means (E and G), or violin plots (F). Statistical analysis used paired (C, E, G, H, and J) or unpaired Student's *t* test (F), where *p < 0.05, **p < 0.01, ***p < 0.001.

See also Figure S2.

expression analysis using microfluidic qRT-PCR (Figure 1G). All individual colonies expressed at least one lineage marker for ductal cells (*KRT19*, *PROM1*, and *MUC1*), over 90% expressed multipotent progenitor markers (*PDX1*, *SOX9*, and *NKX6.1*), and over 70% expressed an acinar marker (*AMY2A*) (Figures 1H and 1I). Markers for endocrine progenitor cells (*NEUROD1* and *NEUROG3*) and endocrine cells (*INS*, *GCG*, *SST*, *PPY*, and *GHRL*) were detected in a subset of colonies (Figures 1H and 1I). Overall, the frequency of individual colonies expressing various lineage markers was not different among colonies grown in 9F + Ri versus 6F + Ri (Figure 1I), suggesting tri-lineage differentiation was not altered in PCFUs cultured in 6F + Ri. Immunofluorescence (IF) staining confirmed protein markers for ductal (KRT19, PanCK), acinar (amylase), endocrine (CHGA), and epithelium (CDH1) in 3-week-old colonies grown in 6F + Ri colony assay (Figures 1J–1L and S2A–S2C). Together, these results indicate that the 6F + Ri colony assay is sufficient for survival, self-renewal, and tri-lineage differentiation of human ductal progenitor-like cells.

Six soluble factors are required for the survival of some exocrine cells that form spheroids in a 3D suspension culture

Next, we sought to determine whether 6F alone, without Matrigel or methylcellulose, is sufficient to support cellular survival in 3D suspension culture. Cryopreserved exocrine cells were thawed and plated in ultra-low adherent culture plates in the presence of 6F for 7 days. Because of the pro-survival effect of Ri on PCFUs (Figure S1B), Ri was added for the first overnight incubation to boost PCFU survival after thawing from cryopreservation (Figure 2A). Extensive cell death was observed on D1 under a phase-contrast light microscope (not shown), while spheroid formation became apparent between D3 and D7 of suspension culture (Figure 2B). To determine whether the 6F are required for suspension cell survival, they were removed from the suspension medium (zero factor, 0F) and cell number determined over time. At D3 and afterward, spheroids were dissociated into a single-cell suspension using Liberase TH followed by TrypLE to aid cell number enumeration. The number of total live cells declined equally with or without the presence of 6F until D3 (Figure 2C). By D7, 20.5 ± 4.2% live cells remained in 6F compared to D0, whereas only 3.4 ± 0.6% live cells remained in 0F, demonstrating the requirement of 6F for the survival of some exocrine cells over time (Figure 2C).

Ductal progenitor-like cells are preserved in 6F suspension culture

The findings that 6F was required to support ductal PCFUs survival and proliferation in our colony assay (Figures 1B and 1C) and that 6F was required for the survival of some exocrine cells in suspension at D7 (Figure 2C) suggest that ductal PCFUs may be enriched in suspension at D7. To test this, D7 spheroids were dissociated into a single-cell suspension and plated into the 6F + Ri colony assay, with freshly thawed D0 cells used as a control (Figure 2D). The colony-forming efficiency was significantly higher in dissociated D7 spheroids compared to D0 cells (Figure 2E); there was no difference in the diameters of 3-week-old colonies (Figure 2F), suggesting PCFUs are enriched following 7 days of suspension culture without loss of their proliferative potential. However, calculated PCFU numbers (total live cells per well in suspension culture multiplied by colony-forming efficiency) declined at D7 compared to D0, indicating sub-optimal survival of progenitor-like cells in suspension culture (Figure 2G). Similar to the results found for D0 PCFUs (Figure 1F), D7 suspension cultured PCFUs maintained self-renewal capacity in 6F + Ri colony assay over 9 weeks (Figure 2H). To compare lineage differentiation capacity of PCFUs, D0 and D7 suspension cells were plated into 6F + Ri colony assay for 3 weeks. The frequency of 3-week-old colonies expressing the three main lineage markers was not different between the colonies derived from D0 versus D7 suspension culture (Figures 2I and 2J), suggesting the maintenance of tri-lineage differentiation capacity of PCFUs over 7 days in suspension culture. Protein markers for ductal (KRT19, PanCK), acinar (amylase), endocrine (CHGA) and epithelium (CDH1) were confirmed in 3-week-old colonies derived from PCFUs in D7 suspension culture (Figures 2K–2M and S2D–S2F). Together, these data demonstrate that the 6F preserves the capacities of self-renewal and tri-lineage differentiation of ductal progenitor-like cells grown in 3D suspension over 7 days, but the condition is suboptimal for survival.

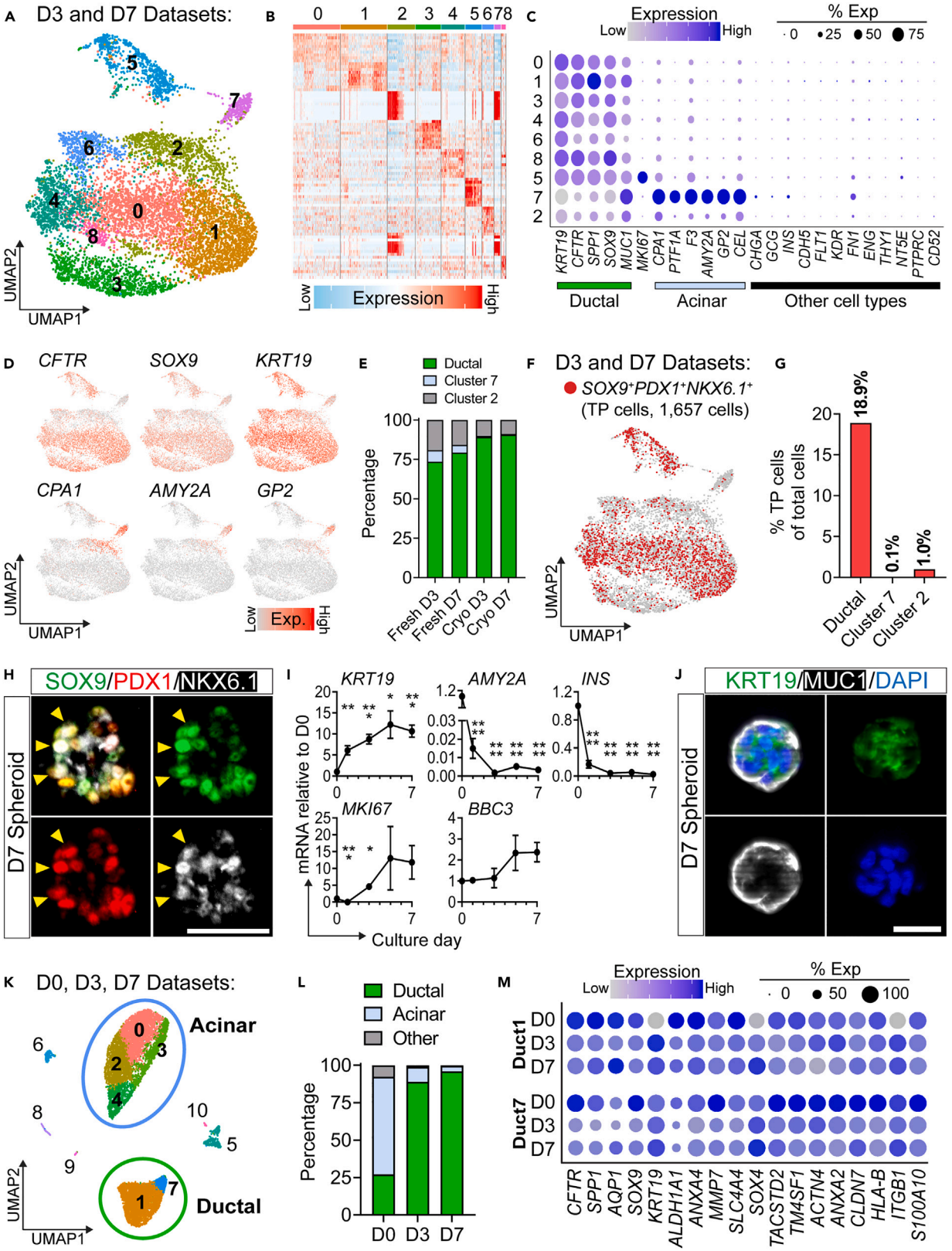
A
D3 and D7 Datasets:
UMAP2
UMAP1
B
0 1 2 3 4 5 6 7 8
Low
Expression
High
C
Expression
Low
High
% Exp
0
25
50
75
KRT19 CFTR SPP1 SOX9 MUC1 MKI67 CPA1 PTF1A F3 AMY2A GP2 CEL CHGA GCG INS CDH5 FLT1 KDR FN1 ENG THY1 NT5E PTPRC CD52
Ductal
Acinar
Other cell types
D
CFTR
SOX9
KRT19
CPA1
AMY2A
GP2
Low
Exp.
High
E
Ductal
Cluster 7
Cluster 2
Percentage
Fresh D3
Fresh D7
Cryo D3
Cryo D7
F
D3 and D7 Datasets:
SOX9+PDX1+NKX6.1+
(TP cells, 1,657 cells)
G
% TP cells of total cells
18.9%
0.1%
1.0%
Ductal
Cluster 7
Cluster 2
H
SOX9/PDX1/NKX6.1
D7 Spheroid
I
KRT19
AMY2A
INS
MKI67
BBC3
mRNA relative to D0
Culture day
J
KRT19/MUC1/DAPI
D7 Spheroid
K
D0, D3, D7 Datasets:
Acinar
Ductal
L
Ductal
Acinar
Other
Percentage
D0 D3 D7
M
Expression
Low
High
% Exp
0
50
100
Duct1
Duct7
D0
D3
D7
CFTR SPP1 AQP1 SOX9 KRT19 ALDH1A1 ANXA4 MMP7 SLC4A4 SOX4 TACSTD2 TM4SF1 ACTN4 ANXA2 CLDN7 HLA-B ITGB1 S100A10

Figure 3. Single-cell RNA-sequencing analysis indicates that most cells cultured in 6F suspension are ductal cells

(A–E) Examination of D3 and D7 suspension culture datasets (N = 2 donors each). (A) UMAP plot of aggregated D3 and D7 suspension cell datasets and (B) cluster-specific gene heatmap. (C) Gene expression dot plots and (D) UMAP plots showing expression of selected ductal and acinar genes. (E) Population percentage analysis of each dataset.

(F–H) Examination of cells that simultaneously express *SOX9*, *PDX1*, and *NKX6.1* (TP cells). (F) UMAP plot of TP cells and (G) their percentage distribution across major cell phenotypes. (H) Representative immunofluorescence (IF) staining of D7 spheroid for SOX9 (green), PDX1 (red), and NKX6.1 (white). Scale bar: 50 μm. Arrow heads indicate TP cells.

(I and J) Validation of ductal cell phenotype of suspension-cultured cells. (I) Conventional qRT-PCR for selected genes during suspension culture, with each timepoint calculated as fold change (FC) relative to D0. Data are depicted as mean ± SEM. N = 3–5 donors per timepoint, 2–3 technical replicates. Statistical analysis was done using paired Student's *t* test comparing all time points against D0, where *p < 0.05, **p < 0.01, ***p < 0.001, and ****p < 0.0001. (J) Representative IF staining of D7 spheroid for KRT19 (green) and MUC1 (white); DAPI was used to visualize nuclei. Scale bar: 50 μm.

(K–M) Comparison of suspension-cultured cells (D3 and D7) and freshly dissociated exocrine tissue (D0). (K) UMAP plot of D0, D3, and D7 datasets and (L) distribution of cell phenotypes in each dataset. (M) Gene expression dot plot of genes up-regulated in D0, D3, and D7 ductal cells (Duct1 and Duct7) compared against all other cell types. Differentially expressed genes (DEGs) from each list (p value < 0.05) were compared, and selected genes presented. See also Figures S2 and S3.

Single-cell RNA-sequencing reveals that most cells in 6F suspension culture are ductal cells

To comprehensively characterize cells grown in the 6F suspension culture, spheroids were dissociated into a single-cell suspension and processed by single-cell RNA-sequencing (scRNA-seq). Cultured cells from cryopreserved and non-cryopreserved (freshly dissociated) exocrine tissue were compared. Following quality control (Figures S3A and S3B), 8,312 cells from four samples (two from D3 and two from D7) were analyzed. Using Principal Component and Uniform Manifold Approximation and Projection (UMAP) dimensional reduction, nine unique clusters were identified (Figures 3A, 3B, S3C, and S3D), with each sample contributing to all nine clusters (Figures S3E and S3F; Table S5).

Based on known lineage markers, seven clusters (0, 1, 3, 4, 5, 6, and 8) exhibited a ductal phenotype (83.7% of total cells; Figures 3C, 3D, and S3D), with cluster 5 expressing high levels of the proliferation marker *MKI67*.[19] Cluster 7 (3.1% of total cells; Figure S3D) displayed mostly an acinar phenotype (Figures 3C and 3D). Further examination revealed that most of the cluster 7 cells originated from the non-cryopreserved samples (Figures 3E, S3E, and S3F), and many acinar markers were absent in the cryopreserved samples (Figures S3G and S3H). Cluster 2 (13.2% of total cells; Figure S2D) expressed low levels of both ductal and acinar markers (Figures 3C and 3D), and like cluster 7, cluster 2 was primarily derived from non-cryopreserved samples (Figure S3F). In contrast, cryopreservation did not alter the expression of canonical ductal markers, *ALDH1A3*, *CFTR*, *KRT19*, *PROM1*, and *SOX9* (Figure S3I), whereas endocrine markers, *NEUROG3*, *INS*, *PPY*, *SST*, and *GHRL*, were minimally expressed by both the cryopreserved and the non-cryopreserved exocrine samples (Figure S3J). These observations suggest that cryopreservation and thawing select against acinar cells among the dissociated exocrine cells.

Acinar cells are known to *trans*-differentiate into a duct-like phenotype *in vivo*,[20] which can be recognized by the expression of *GP2*, *F3* (CD142), and *MECOM* in a culture initiated with non-dissociated human exocrine tissue[21,22]; however, these *trans*-differentiation markers were minimal in the cryopreserved compared to the non-cryopreserved samples (Figures S3G and S3H). These data suggest that acinar-to-ductal *trans*-differentiation may not account for most of the ductal cells grown in our 6F suspension culture, especially those originated from the cryopreserved samples.

Previously, we found that a sub-population of ductal cells in endogenous adult human pancreas simultaneously expresses the embryonic multipotent progenitor cell markers SOX9, PDX1, and NKX6.1.[12] These triple-positive (TP) cells were also present in D3 and D7 suspension cells (Figures 3F and S3K). The percentage of TP cells among freshly dissociated exocrine cells were 3.6%[12] and 18.9% among all analyzed suspension cells (Figure 3G), which are within the colony-forming efficiency range of D0 and D7 cells, respectively (Figure 2E). Protein expression of SOX9, PDX1, and NKX6.1 in D7 spheroids confirmed a sub-population of cells that co-expressed all three markers (Figure 3H, yellow arrowheads, and S2G). Together, these results demonstrate that cells in suspension contain a heterogeneous mixture of both ductal progenitor-like and ductal non-progenitor cells.

Conventional qRT-PCR validated that expression of acinar (*AMY2A*) and endocrine (*INS*) markers decreased by D1. In contrast, ductal marker (*KRT19*) expression increased over time (Figure 3I), and protein expression of KRT19 and MUC1 (an apical marker of ductal cells[23]) were confirmed in D7 spheroids (Figure 3J and S2H).

To determine whether suspension-cultured ductal cells are comparable to freshly dissociated ductal cells at the transcriptomic level, datasets from D3 and D7 suspension cells were projected onto scRNA-seq data of D0 cells[12] and compared (Figure 3K; Table S5). The majority of D3 and D7 suspension cells co-localized with two D0 ductal clusters: "Duct1" and "Duct7" (Figures 3K and 3L). Expression patterns for canonical ductal and ductal cell-enriched markers[24] were comparable between D0, D3, and D7 for Duct1 and Duct7 clusters (Figure 3M), suggesting ductal identity is preserved in suspension culture.

Apical-basal polarization is promoted by 5% (v/v) Matrigel in 6F suspension culture, resulting in cystic structure formation

MUC1 was expressed on the outer layer of D7 spheroids (Figure 3J), typical of an apical-out polarity previously reported in suspension cultures of epithelial cells.[25,26] Signaling from ECM protein engagement is required for the formation of proper epithelial cell apical-basal polarity, and can improve epithelial cell survival and function.[27] We therefore examined the effects of ECM proteins on suspension cells. To avoid the confounding effects of stiffness brought by high concentrations of Matrigel,[14,28] a low concentration (5% v/v) of Matrigel was added to D1 suspension cells (Figure 4A). This low concentration of Matrigel was sufficient to induce the formation of cystic structures (Figure 4B), similar to

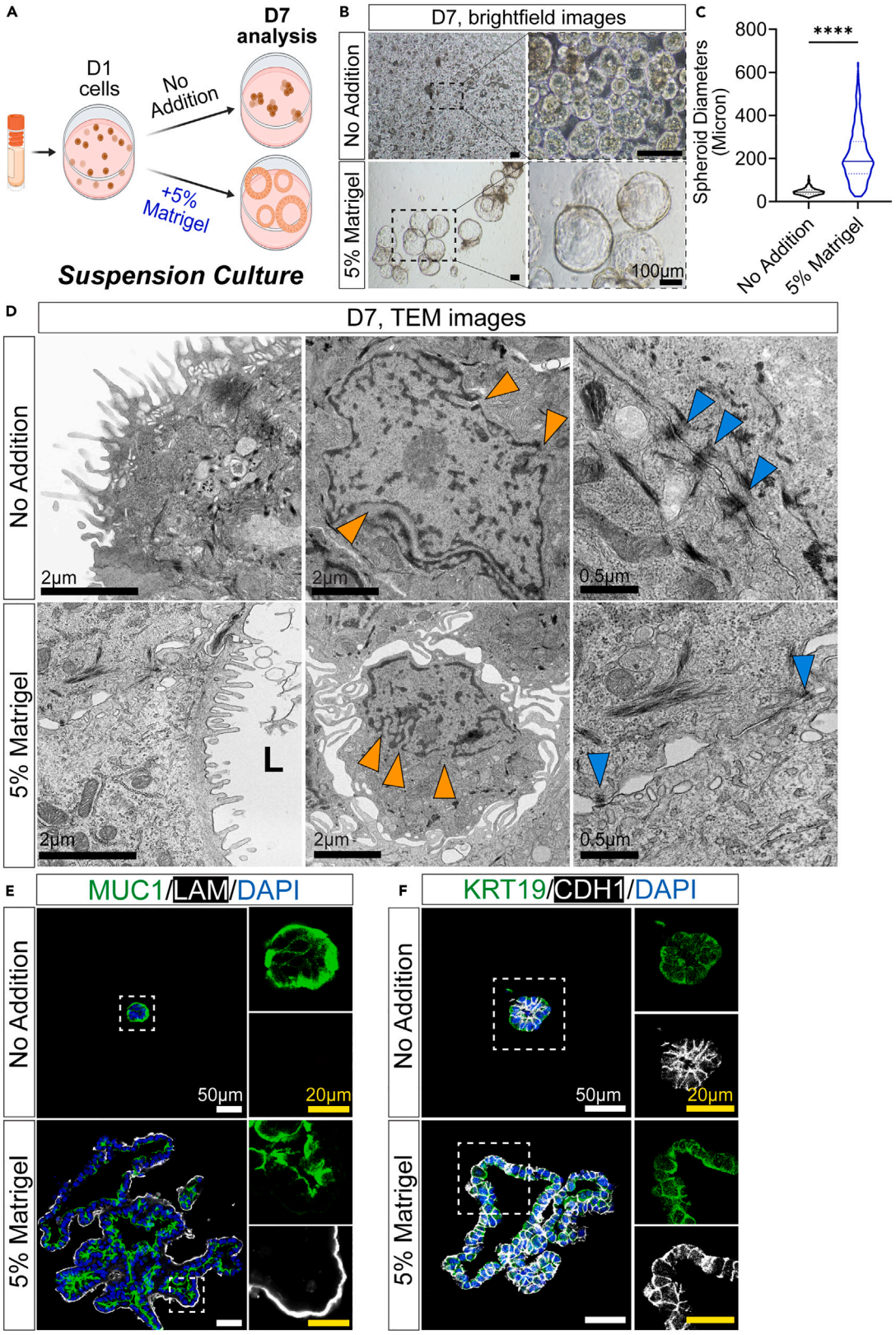
A
D7
analysis
D1
cells
No
Addition
+5%
Matrigel
Suspension Culture
B
D7, brightfield images
No Addition
5% Matrigel
100μm
C
Spheroid Diameters
(Micron)
800
600
400
200
0
****
No Addition
5% Matrigel
D
D7, TEM images
No Addition
5% Matrigel
2μm
2μm
0.5μm
L
2μm
2μm
0.5μm
E
MUC1/LAM/DAPI
No Addition
5% Matrigel
50μm
20μm
F
KRT19/CDH1/DAPI
No Addition
5% Matrigel
50μm
20μm

Figure 4. Addition of 5% Matrigel to suspension culture drives ductal cell apical-basal polarization

(A) Schematic for suspension culture using 5% Matrigel.

(B) Representative brightfield images of D7 spheroids cultured with or without 5% Matrigel. Scale bars: 100 μm.

(C) D7 spheroid/cyst diameter measurements. N = 3 donors, n = 30–100 spheroids/cysts. Statistical analysis was done using unpaired Student's *t* test with Welch's correction, where ****$p < 0.0001$.

(D) Transmission electron microscopy (TEM) images of D7 cells cultured with or without 5% Matrigel. "L" indicates lumen, orange arrowheads indicate nuclear invaginations, and blue arrowheads indicate tight junctions. Scale bars: 2 μm and 0.5 μm.

(E) Representative IF staining of D7 spheroids/cysts for apical (MUC1) and basal (LAM) markers. DAPI was used to visualize nuclei. Scale bars: 50 μm (white) and 20 μm (yellow).

(F) Representative IF staining of D7 spheroids/cysts for ductal (KRT19) and cell border (CDH1) markers. DAPI was used to visualize nuclei. Scale bars: 50 μm (white) and 20 μm (yellow).

See also Figures S2 and S4.

that described for colonies[12] and organoids.[9,10] At D7, the diameters of cysts reached 211.9 ± 119.5 μm in the presence of 5% Matrigel, compared to the no addition control spheroids at 47.1 ± 15.8 μm (Figure 4C). Transmission electron microscopy (TEM) analysis of control D7 spheroids showed microvilli facing outwards, whereas D7 cysts showed microvilli facing the lumen (Figures 4D and S4). Both D7 samples showed invaginated nuclei (Figure 4D, orange arrowheads) and tight junctions (Figure 4D, blue arrowheads), consistent with a ductal phenotype.[29,30] Co-immunofluorescence staining of laminin (LAM; a basement membrane ECM protein[31]) and MUC1 confirmed a lack of LAM-positive basement membrane in control D7 spheroids, whereas a LAM-positive basement membrane and MUC1 localization in the lumen was observed in cysts confirming polarization (Figures 4E and S2I). Additionally, cells cultured in 5% Matrigel continued to express protein markers for ductal (KRT19) and epithelium (CDH1) (Figures 4F and S2J). These results demonstrate that 5% Matrigel induces the formation of ductal cysts with proper apical-basal polarization.

5% (v/v) Matrigel enhances proliferation and decreases apoptosis in 6F suspension culture

In addition to polarity, ECM protein signaling is also known to impact survival, proliferation, and apoptosis.[32] Consistently, conventional qRT-PCR analysis of cells incubated with 5% Matrigel for 24 h showed enhanced expression of proliferation markers (*MKI67*, *CCND1*) and decreased expression of cell cycle inhibitor (*CDKN1A*) and apoptotic (*BBC3*) markers compared to the no addition controls (Figure 5A), demonstrating the acute effects of Matrigel. Additionally, by D7 of suspension culture, total live cell numbers were increased by 5.2 ± 1.9-fold in 5% Matrigel compared to the no addition control (Figure 5B).

To determine whether PCFUs are affected by Matrigel, D7 cells treated with and without 5% Matrigel were dissociated and plated into 6F + Ri colony assay, and the resulting 3-week-old colonies counted. The colony-forming efficiency was unchanged (Figure 5C), while the total PCFU number increased by 4.3 ± 0.9-fold compared to the no addition control (Figure 5D). However, colony diameters were smaller in colonies derived from the D7 PCFUs cultured with 5% Matrigel compared to no addition control (Figure 5E), demonstrating a reduced proliferative potential. Overall, these results indicate that PCFUs expand in Matrigel-supplemented suspension culture, but at the expense of their proliferative capacity.

Markers for both proliferation (*MKI67*) and apoptosis (*BBC3*) increased over time in 6F suspension culture (Figure 3I). When lacking appropriate stimuli, proliferating cells can be arrested during the cell cycle and undergo apoptosis.[33,34] To test this possibility, we first analyzed the cell-cycle status of the suspension cells at D7 of culture using KI67 (expressed from late G1 through M phase) and a thymidine analogue EdU (labels newly synthesized DNA strands) (Figures 5F and 5G). As expected, EdU labeled most of the actively replicating $KI67^+$ cells (87.8 ± 23.9% of cells in no addition control and 94.0 ± 9.6% of cells in 5% Matrigel) (Figure S5A). Among total cells, the no addition control contained 26.1 ± 20.9% $KI67^+$ cells, whereas addition of 5% Matrigel increased $KI67^+$ cells to 45.5 ± 20.8% (Figure 5G, top), confirming that Matrigel is inducing active proliferation. A small percentage of EdU^+KI67^- cells, indicative of cells that completed cell cycle, was detected in the no addition control (0.2 ± 1.1%) and increased following the addition of 5% Matrigel (4.7 ± 4.0%) (Figure 5G, bottom). To investigate the impact of 5% Matrigel on apoptosis, we next examined cleaved caspase 3 ($CC3$[35,36]) expression (Figures 5H and 5I). The no addition control had 17.1 ± 13.3% $CC3^+$ cells per total cells, whereas with 5% Matrigel the percentage was reduced to 4.2 ± 5.1% (Figure 5I, top). Furthermore, 5% Matrigel addition decreased the percentage of $CC3^+KI67^+$ cells among $KI67^+$ cells (3.3 ± 5.0%) compared to the no addition control (29.4 ± 32.0%) (Figure 5I, bottom). Taken together, these results demonstrate that ductal cells in suspension culture can enter the cell cycle but fail to complete mitosis and become apoptotic, whereas the addition of 5% Matrigel promotes completion of the cell cycle and reduces apoptosis.

Bulk transcriptomic analysis indicates enhanced cellular activation pathways in cells stimulated with 5% Matrigel

To gain further insights of the effects of 5% Matrigel, global gene expression was examined using bulk mRNA-sequencing. Principal component analysis (PCA) confirmed the dissimilarity of overall gene expression patterns between samples treated with or without 5% Matrigel (Figure 5J). Overall, 1,036 differentially expressed genes (DEGs) were identified (Figures 5K and S5B; Table S6). Pathway analysis using gene set enrichment analysis (GSEA) with databases from Hallmark (Figure 5L), Kyoto Encyclopedia of Genes and Genomes (KEGG), and Gene Ontology-Biological Processes (GO-BP) (Figures S5C and S5D) revealed that, compared to the no addition control, cells cultured with 5% Matrigel expressed more genes related to metabolism (e.g., glycolysis, oxidative phosphorylation, fatty acid metabolism, and ATP metabolic process) and cell cycle (e.g., G2M checkpoint, DNA replication, and mismatch repair) (Table S6). In contrast, no addition control cells were

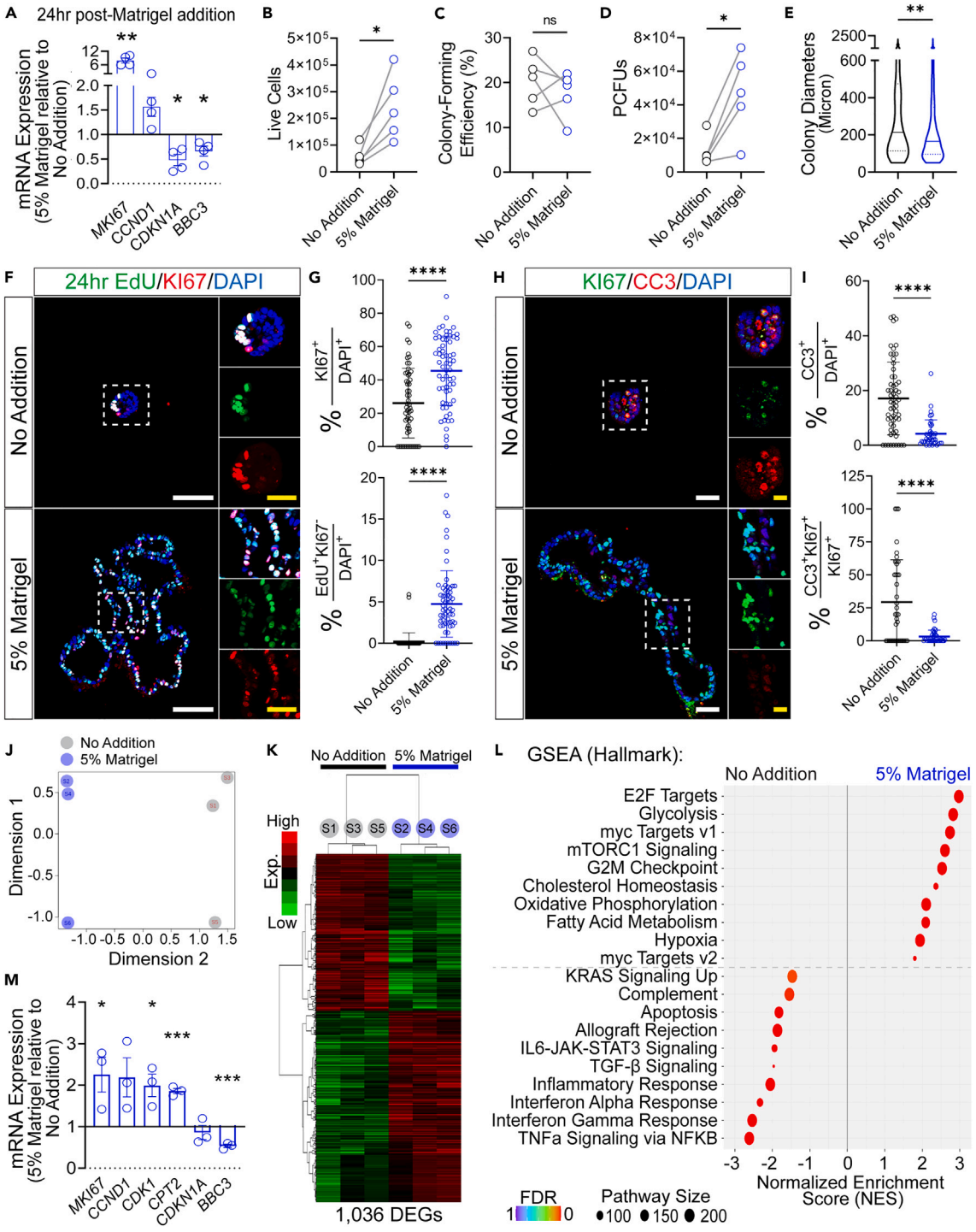

Figure 5. Addition of 5% Matrigel to suspension culture drives cellular expansion by increasing proliferation and decreasing apoptosis

(A) Conventional qRT-PCR analysis of suspension cells 24 h following addition of 5% Matrigel on D1 cells, shown as fold change relative to no addition controls. (B–E) Comparison of 5% Matrigel and no addition conditions in suspension culture. (B) Total live cells at D7. (C) Colony-forming efficiency quantification. (D) PCFU quantification. (E) Colony diameter measurements. 500 or 1,000 cells plated per well. Data are depicted as mean ± SEM. N = 5 donors; (C and D) n = 2–4 technical replicates, (E) 45–50 individual colonies.

(F–G) Representative IF staining and quantification of D7 cell cycle analysis. (F) Cells were stained using EdU (5-ethynyl-2′-deoxyuridine; green), KI67 (red), and DAPI. (G) Quantification of percentages of actively proliferating cells (top; $KI67^{+}/DAPI^{+}$) and cells that completed the cell cycle (bottom; $EdU^{+}KI67^{-}/DAPI^{+}$) per section. N = 3 donors, n = 10–22 individual images. Scale bars: 50 μm (white) and 20 μm (yellow).

Figure 5. *Continued*

(H and I) Representative IF staining and quantification of D7 cells for apoptosis analysis. (H) Cells were stained using KI67 (green), cleaved caspase 3 (CC3; red), and DAPI. (I) Quantification of percentages of apoptotic cells (top; $CC3^+/DAPI^+$) and proliferative cells undergoing apoptosis (bottom; $CC3^+KI67^+/KI67^+$) per section. N = 3 donors, n = 10–21 individual spheroid images. Scale bars: 50 μm (white) and 20 μm (yellow).

(J–L) Bulk mRNA-sequencing of D7 cells cultured with or without 5% Matrigel from three donors. (J) Principal Component Analysis plot, where gray dots indicate no addition controls and blue dots indicate 5% Matrigel samples. (K) Heatmap of 1,036 differentially expressed genes (DEGs). (L) Gene set enrichment analysis (GSEA) from the Hallmark molecular signature database (top pathways shown, FDR < 0.05).

(M) Conventional qRT-PCR of selected DEGs comparing 5% Matrigel-treated cells relative to no addition controls. N = 3 donors, n = 3 technical replicates. Data are depicted as mean ± SEM (A and M), donor means (B–D), violin plots (E), or mean ± SD (G and I). Statistical analysis used paired Student's *t* test (A–D and M) or unpaired Student's *t* test with Welch's correction (E, G, and I), where *p < 0.05, **p < 0.01, ***p < 0.001, and ****p < 0.0001.

See also Figure S5.

enriched for genes associated with inflammatory (e.g., complement, allograft rejection, and interferon response) and apoptosis pathways. The proliferation and apoptosis pathways were consistent with the immunostaining results (Figures 5F–5I). Further validation using conventional qRT-PCR demonstrated up-regulation of proliferation (*MKI67*, *CCND1*, and *CDK1*) and metabolic (*CPT2*) markers and down-regulation of senescence (*CDKN1A*) and apoptosis (*BBC3*) markers in D7 cells treated with 5% Matrigel compared to the no addition control (Figures 5M and S5B). Interestingly, pathways for tight junction and focal adhesion assembly were enriched in the no addition control in the KEGG and GO-BP analysis, respectively (Table S6), consistent with the TEM analysis showing minimum intercellular space in the no addition controls compared to the Matrigel treated group (Figures 4D and S4). Together, these results indicate that Matrigel up-regulates pathways in metabolism and proliferation and down-regulates cell-cell contact in suspension culture.

Collagen IV increases adenosine triphosphate (ATP) production, cell numbers, and cyst formation in 6F suspension culture

Matrigel comprises over 1,800 unique proteins, with the majority by mass being ECM proteins such as laminins and collagens.[13] We sought to identify specific ECM proteins that mimic the effects of 5% Matrigel. A screening array printed with 36 conditions containing 1 to 4 ECM proteins or the vehicle bovine serum albumin (BSA) (Figure S6A) was seeded with D1 cells and incubated for 24 h with gentle rocking (Figure 6A). Compared to the negative control, suspension cells preferentially adhered to ten ECM protein conditions (Figure 6B). Individually, collagen IV, collagen VI, and vitronectin were sufficient for suspension cell adherence (Figure 6B); therefore, these three ECM proteins were examined in subsequent experiments.

The proliferation and metabolism pathways identified in the bulk RNA-seq analysis of cells cultured in 5% Matrigel (Figures 5L, S5C, and S5D) prompted us to examine whether intracellular ATP, which is required for cell proliferation and metabolism,[37] was increased following culture in the presence of ECM proteins (Figure 6C). ATP production was increased with the addition of 5% Matrigel and collagen IV compared to the no addition control (Figure 6D) but was unaffected following culture with collagen VI and vitronectin (Figure S6B). Additionally, diameters of D7 cysts increased in the presence of collagen IV in a dose-dependent manner (Figures 6E, 6F, and S6C). In a time-course analysis, an increase in ATP production was observed between days 3–6 post-collagen IV addition compared to cells prior to treatment (Figure 6G). Finally, total cell numbers increased by 2.0 ± 0.4-fold in D7 suspension cells cultured for 6 days with collagen IV compared to the control (Figure 6H). Together, these data identify collagen IV as an ECM protein that mimics the effects of 5% Matrigel on suspension cells.

Collagen IV stimulates ductal progenitor-like cell survival and proliferation in methylcellulose colony assay

We next determined whether collagen IV can replace 5% Matrigel in the 6F + Ri colony assay to support the survival of CD133-enriched ductal progenitor-like cells[12] (Figures 6I and S6D). In the absence of ECM proteins only 0.15 ± 0.04% of plated CD133+ ductal cells formed colonies, whereas in the presence of 5% Matrigel 12.1 ± 1.2% formed colonies (Figure 6J). Collagen IV at a low dose (10 μg/mL) resulted in 0.6 ± 0.1% colony-forming efficiency, and the two higher doses (100 and 200 μg/mL) both increased the efficiency to 3.2 ± 0.4% (Figure 6J), indicating that collagen IV has a dose-dependent effect on PCFU survival. The diameters of 3-week-old colonies cultured with collagen IV also increased in a dose-dependent manner (Figure 6K). Overall, these results indicate that collagen IV is sufficient to stimulate the survival and proliferation of some ductal progenitor-like cells, although Matrigel out-performs collagen IV in the colony assay.

The effects of collagen IV and Matrigel on suspension cells are mediated through integrin receptor α1β1

Of the known collagen-specific integrin receptors, collagen IV preferentially binds to and activates the heterodimerized integrin receptor α1β1.[38,39] To investigate whether the effects of collagen IV are mediated through the integrin α1β1 receptor, we first blocked the integrin β1 subunit with an anti-β1 antibody[40,41] (Figure 7A). As expected, ATP production was increased in collagen IV-stimulated culture at D7 compared to no addition control (Figure 7B). Addition of the anti-β1, but not the isotype control antibody, reduced ATP production in a dose-dependent manner in the presence of collagen IV (Figures 7B and S7A). Likewise, blocking the integrin α1 subunit with an anti-α1 antibody[42,43] reduced ATP production in a dose-dependent manner in the presence of collagen IV (Figures 7C and S7A). These results demonstrate that integrin receptor α1β1 signaling is required to mediate the effects of collagen IV on ATP production in suspension culture.

Next, we examined the impact of integrin receptor α1β1 signaling on suspension cell survival (Figures 7D and 7E). Compared to isotype control, addition of the anti-α1 antibody reduced the number of live cells (Figure 7F) and cyst diameters (Figure 7G) in D7 cells cultured in the

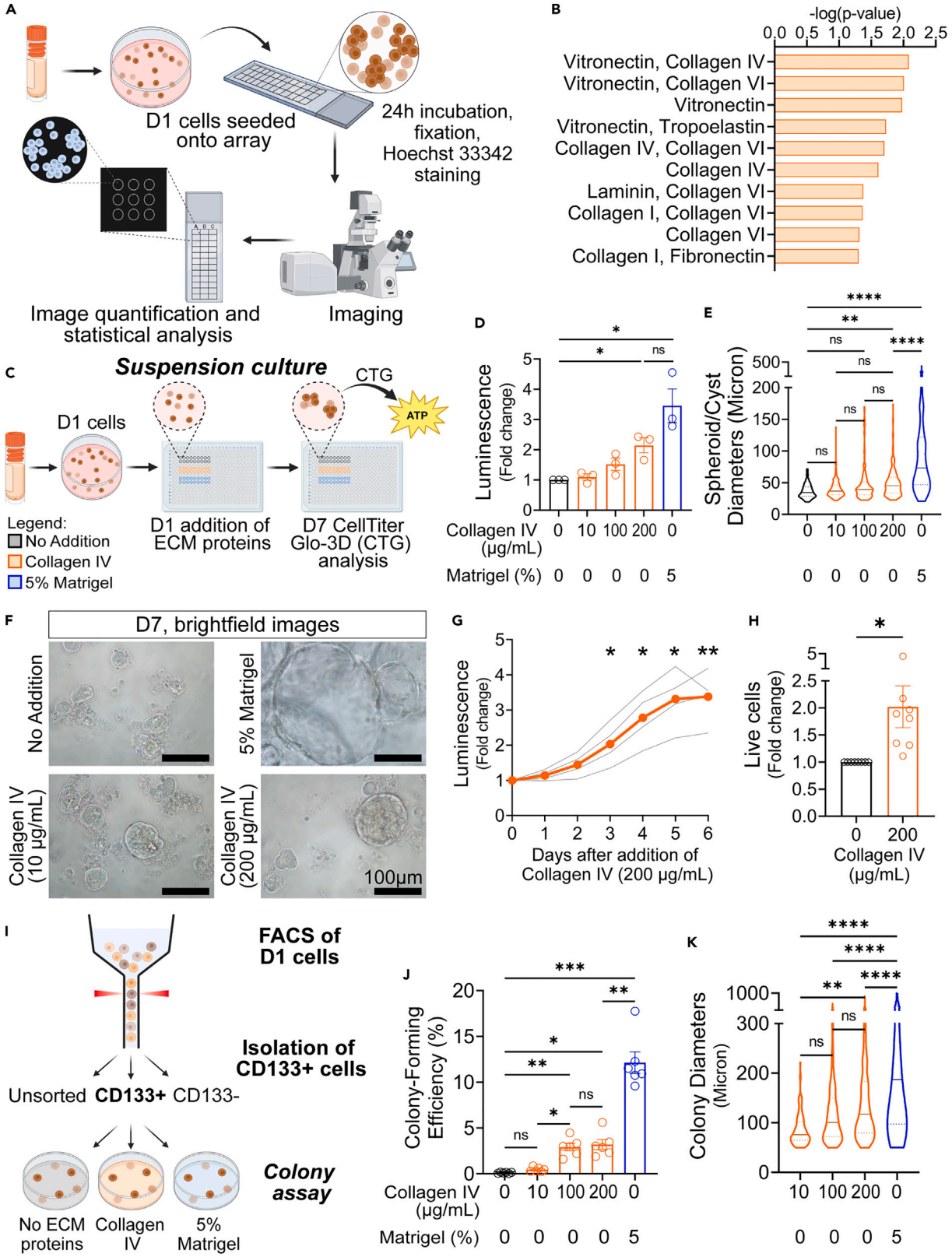
A
D1 cells seeded onto array
24h incubation, fixation, Hoechst 33342 staining
Imaging
Image quantification and statistical analysis
B
-log(p-value)
0.0 0.5 1.0 1.5 2.0 2.5
Vitronectin, Collagen IV
Vitronectin, Collagen VI
Vitronectin
Vitronectin, Tropoelastin
Collagen IV, Collagen VI
Collagen IV
Laminin, Collagen VI
Collagen I, Collagen VI
Collagen VI
Collagen I, Fibronectin
C
Suspension culture
CTG
ATP
D1 cells
D1 addition of ECM proteins
D7 CellTiter Glo-3D (CTG) analysis
Legend:
No Addition
Collagen IV
5% Matrigel
D
Luminescence (Fold change)
Collagen IV (µg/mL) 0 10 100 200 0
Matrigel (%) 0 0 0 0 5
E
Spheroid/Cyst Diameters (Micron)
F
D7, brightfield images
No Addition
5% Matrigel
Collagen IV (10 µg/mL)
Collagen IV (200 µg/mL)
100µm
G
Luminescence (Fold change)
Days after addition of Collagen IV (200 µg/mL)
H
Live cells (Fold change)
Collagen IV (µg/mL)
I
FACS of D1 cells
Isolation of CD133+ cells
Unsorted CD133+ CD133-
Colony assay
No ECM proteins
Collagen IV
5% Matrigel
J
Colony-Forming Efficiency (%)
K
Colony Diameters (Micron)

Figure 6. Collagen IV promotes the survival and activation of ductal progenitor-like cells

(A) Schematic for ECM protein array experiment.

(B) Significant ECM protein combinations adhered to by suspension cells. N = 4 donors.

(C) Experimental schematic for ECM protein addition to suspension culture.

(D–F) D7 analysis after culture with or without collagen IV or 5% Matrigel. (D) Adenosine triphosphate (ATP) produced by D7 cells relative to no addition control, and (E) spheroid/cyst diameter measurements. (F) Representative brightfield images. N = 3 donors, (D) n = 2 technical replicates, (E) 50–100 individual spheroids/cysts. Scale bars: 100 μm.

(G) Fold-change quantification of ATP produced by cells during time course following 200 μg/mL collagen IV addition, relative to 0 days after collagen IV addition. N = 4 donors (gray lines), n = 2 technical replicates.

(H) Fold-change quantification of cell numbers at D7 following culture with collagen IV relative to the no addition control. N = 8 donors, n = 2 technical replicates.

(I–K) CD133+ ductal progenitor cell plating in colony assay supplemented with or without collagen IV or 5% Matrigel. (I) Experimental schematic, (J) colony-forming efficiency quantification, and (K) colony diameter measurements following culture in colony assay. N = 6 donors; (J) n = 4 technical replicates, (K) 20–50 individual colonies. Data are depicted as donor means (B and G), mean ± SEM (D, H, and J), or violin plots (E and K). Statistical analyses used paired Student's *t* test (B, D, G, H, and J) or one-way ANOVA with Tukey's correction (E and K), where *p < 0.5, **p < 0.01, ***p < 0.001, and ****p < 0.0001.

See also Figure S6.

presence of collagen IV (orange) or 5% Matrigel (blue). In the absence of ECM proteins, the live cell counts and diameters of cysts were unaffected by the addition of anti-α1 antibodies (Figure S7B), which indicates that anti-α1 antibody by itself is not toxic to the suspension cells.

To assess PCFU survival, suspension cells cultured in the presence of collagen IV or Matrigel were incubated with isotype or anti-α1 antibodies, and the resulting D7 cells were plated into the 6F + Ri colony assay for 3 weeks (Figure 7H). Compared to the isotype control, addition of the anti-α1 antibody reduced both the colony-forming efficiency (Figure 7I) and total PCFU numbers (Figure 7J) in D7 suspension culture, whereas the colony diameters were unaffected (Figure 7K), suggesting that survival but not proliferative potential of PCFUs is blocked by anti-α1 antibody. Taken together, these results indicate that integrin receptor α1β1 signaling is necessary to mediate the effects of collagen IV and 5% Matrigel on ductal progenitor-like cells in suspension culture.

DISCUSSION

Matrigel impacts cells using cell surface receptor signaling via integrin receptors and mechanical stimulation via its stiffness.[14,44] To reduce the confounding effects inherent in highly concentrated Matrigel, we demonstrate here that a low concentration of Matrigel is sufficient to stimulate survival, activation, polarization, and expansion of primary pancreatic ductal progenitor-like and ductal non-progenitor cells from cadaveric donors without apparent diseases. Our results are consistent with several recent reports demonstrating that low concentrations of Matrigel are adequate to enhance the survival and activation of adult primary intestine, mammary, and liver cells.[45–49] Furthermore, to the best of our knowledge, our results are the first to show that human ductal progenitor-like and ductal non-progenitor cells require integrin receptor α1β1 signaling to mediate the effects of ECM proteins such as Matrigel and collagen IV.

ECM protein signals establish epithelial cell polarity.[27] Consequently, an apical-out morphology is found when intestinal organoids are cleaned of Matrigel and replated into 3D suspension culture[25] or when induced pluripotent cell-derived intestinal cells are cultured in suspension.[50] Our results are consistent in that pancreatic ductal spheroids have an apical-out morphology when cultured in suspension, which became apical-in after stimulation with 5% Matrigel (Figure 4). Epithelial cells also require ECM protein signals to prevent anoikis,[51–53] a type of apoptosis that can occur due to cellular detachment from the ECM. Here, we find that ductal spheroids have higher proportions of cells undergoing apoptosis compared to those treated with 5% Matrigel (Figure 5). Finally, ECM proteins are known to stimulate epithelial cell proliferation via integrin receptor signaling cascades.[54,55] Consistently, we find that survival and expansion of ductal progenitor-like and ductal non-progenitor cells are enhanced by ECM proteins (Figure 6), which is dependent on integrin receptor α1β1 signaling (Figure 7).

A key finding from our study is that collagen IV can recapitulate the effects of 5% Matrigel on ductal progenitor-like cells, albeit with a lower efficacy. This reduced efficacy is not surprising because cellular interactions with ECM proteins are complex and dynamic, and multiple ECM proteins, such as those present in Matrigel,[13] are likely required to provide optimal signaling to cells.[56,57] Collagen IV is unique among collagens as it localizes specifically to the basement membrane of various epithelial cells,[38] including pancreatic exocrine,[58] endocrine,[59,60] and ductal[41] cells. Collagen IV also enhances islet cell survival and function *in vitro*.[59] To the best of our knowledge, our study provides the first functional evidence that collagen IV enhances survival and activation of ductal progenitor-like and ductal non-progenitor cells from the normal adult human pancreas *ex vivo*.

Another key finding of our study is the identification of six soluble factors (nicotinamide, EGF, Noggin, RSPO1, A83-01, and gastrin) that are necessary and sufficient to support the survival of primary human ductal progenitor-like and ductal non-progenitor cells in a defined 3D suspension culture system over 7 days. Although previous reports had employed a serum-free 3D "pancreatospheres" suspension culture,[61–63] in which the resulting pancreatic progenitor cells differentiated into endocrine, acinar, and neuronal cell lineages, ductal lineage potential was not reported. In contrast, spheroids grown in our suspension culture have the potential for endocrine, acinar, and ductal lineage cells (Figures 2I–2M). Because our Matrigel-free suspension and the pancreatosphere suspension utilize different culture conditions, additional studies will be necessary to directly compare the cells grown in the two conditions.

A 3D suspension culture system was also used to culture non-dissociated exocrine tissues from adult human pancreas[21,22]; however, bovine serum was included. In this system, acinar cells were found to de-differentiate into ductal-like cells within 4 days of culture. Although we cannot rule out the possibility of acinar de-differentiation in our suspension culture, especially in the non-cryopreserved samples, it is likely

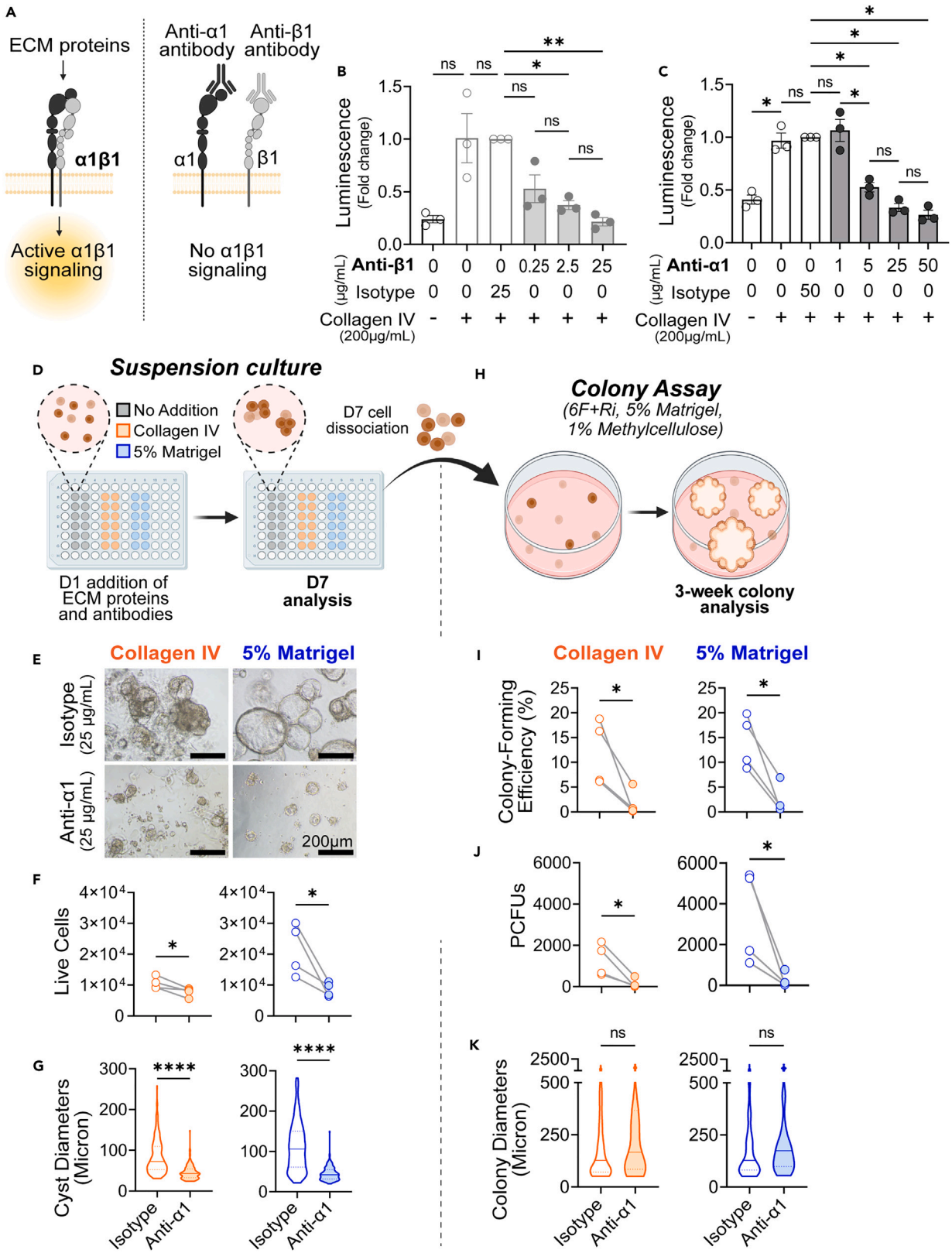
A
ECM proteins
α1β1
Active α1β1 signaling
Anti-α1 antibody
Anti-β1 antibody
α1
β1
No α1β1 signaling
B
Luminescence (Fold change)
Anti-β1 (μg/mL)
Isotype
Collagen IV (200μg/mL)
C
Anti-α1
D
Suspension culture
No Addition
Collagen IV
5% Matrigel
D7 cell dissociation
D1 addition of ECM proteins and antibodies
D7 analysis
H
Colony Assay
(6F+Ri, 5% Matrigel, 1% Methylcellulose)
3-week colony analysis
E
Collagen IV
5% Matrigel
Isotype (25 μg/mL)
Anti-α1 (25 μg/mL)
200μm
I
Colony-Forming Efficiency (%)
J
PCFUs
F
Live Cells
G
Cyst Diameters (Micron)
K
Colony Diameters (Micron)

Figure 7. Integrin receptor α1β1 activity is necessary for ECM protein-mediated ductal progenitor-like cell survival in suspension culture

(A) Integrin α1 blocking antibody schematic.

(B and C) Fold-change quantification of ATP produced by D7 cells cultured with or without an integrin blocking antibody in the presence or absence of 200 μg/mL collagen IV, relative to the isotype control. Cells were cultured in the presence of (B) an integrin β1 blocking antibody (Anti-β1), or (C) an integrin α1 blocking antibody (Anti-α1). N = 3 donors, n = 2 technical replicates.

(D) Experimental schematic of integrin α1 blocking in the presence or absence of ECM proteins for D7 analysis.

(E–G) D7 cell analysis. (E) Representative brightfield images following culture with isotype or anti-α1 antibodies in the presence of 200 μg/mL collagen IV or 5% Matrigel. (F) Total live cells and (G) cyst diameters. N = 4 donors; (F) n = 2 technical replicates, (G) 50–100 cyst diameters. Scale bars: 200 μm.

(H) Experimental schematic of D7 cell dissociation and replating into 5% Matrigel-containing colony assay.

(I–K) Colony assay analysis. Quantification of (I) colony-forming efficiency, (J) PCFU counts, and (K) colony diameter measurements. N = 4 donors, (I and J) n = 4 technical replicates, (K) 45–50 colony diameters. Data are depicted as mean ± SEM (B and C), donor means (F, I, and J), or as violin plots (G and K). Statistical analyses used paired Student's *t* test (F, I, and J), unpaired Student's *t* test with Welch's correction (G and K), or one-way ANOVA with Tukey's correction (B and C), where *p < 0.05 and ****p < 0.0001.

See also Figure S7.

a minor event based on the following observations. First, we routinely dissociate human exocrine tissue into single-cell suspensions using collagenase B.[12] Although acinar and ductal cells make up 70–80% and 10–20% of the exocrine tissue, respectively,[64] ductal cells enrich to 36.2 ± 3.5% among total dissociated D0 exocrine cells.[12] This suggests that dissociation of exocrine tissue selects against acinar cells. Second, the percentage of acinar cells among total D3 or D7 suspension cells—identified in clusters 2 and 7 in our scRNA-seq analysis—is lower in cryopreserved cells compared to non-cryopreserved cells (Figures S3E–S3H), suggesting that cryopreservation further selects against acinar cells. This is additionally supported by the finding that the acinar-to-ductal *trans*-differentiation markers, *F3*, *GP2*, and *MECOM* (Ref), were absent in the cryopreserved sample (Figures S3G and S3H). Finally, we did not detect zymogen granules[29,65]—a key feature of acinar cells—in D7 cells cultured with or without 5% Matrigel in our TEM analysis.

We have previously shown that sequential stimulation of adult human ductal progenitor-like cells with 5% Matrigel and 9F in methylcellulose colony assay for 10 days followed by the addition of a Notch signaling inhibitor, DAPT, can significantly increase the expression of NEUROG3 in 3-week-old colonies, compared to colonies that receive vehicle control. The DAPT-treated NEUROG3$^+$ colonies rescued some of the insulin-dependent diabetic mice 4-months post-transplantation.[12] However, in our suspension culture, 6F alone (Figure S3J), the addition of 5% Matrigel to 6F (Table S6), or the addition of DAPT to 6F (not shown) were all not sufficient to induce NEUROG3 expression. Thus, although the adult human ductal progenitor-like cells grown in 6F suspension culture over 7 days retain both self-renewal and tri-lineage differentiation capacity in our colony assay (Figure 2), it remains unknown what signaling is required to induce NEUROG3 during culture in the suspension platform.

In summary, we have established a well-defined, 3D suspension culture system that allows for the survival of primary ductal progenitor-like and ductal non-progenitor cells from normal human pancreas. Using this suspension platform, we identified Matrigel and collagen IV as positive regulators that act through integrin receptor α1β1 to promote the survival, polarization, and proliferation of human ductal progenitor-like and ductal non-progenitor cells. A suspension platform has facilitated larger scale production of beta-like cells derived from the pluripotent stem cells,[66,67] which has led to a recent clinical trial for the treatment of type 1 diabetes (clinicaltrials.gov: NCT04786262). Because human ductal progenitor-like cells also have potential in regenerative medicine,[12] and Matrigel is unfavorable for clinical applications,[68] the identification of collagen IV in our current study has implications as a first step toward clinical application of these cells for the treatment of diabetes.

Limitations of the study

A defined 3D suspension culture that supports adult human pancreatic ductal progenitor-like cell survival allows for investigation into key mechanisms that control their activities. Although this study demonstrates that collagen IV and integrin receptor α1β1 signaling are necessary for adult human ductal progenitor-like cell survival and activation, it is unknown whether these factors similarly affect endogenous pancreatic ductal progenitor cells. Future efforts to locate and study endogenous ductal progenitors will be necessary to address this question. Another limitation is that not all of the ductal progenitor-like cells survive in the current suspension culture platform without ECM proteins, indicating a need for further optimization.

STAR★METHODS

Detailed methods are provided in the online version of this paper and include the following:

- KEY RESOURCES TABLE
- RESOURCE AVAILABILITY
  - Lead contact
  - Materials availability
  - Data and code availability
- EXPERIMENTAL MODEL AND STUDY PARTICIPANT DETAILS
- METHOD DETAILS
  - Primary tissue single-cell suspension preparation

- Cryopreservation of primary tissue
- 3-Dimensional (3D) colony assay
- Self-renewal colony assay
- 3D suspension culture
- Microfluidic and conventional quantitative (q)RT-PCR
- Immunofluorescence staining
- Preparation of samples for single-cell RNA sequencing
- Computational analysis of single-cell RNA sequencing data
- Bulk mRNA-sequencing
- Electron microscopy
- ECM protein chip array
- Fluorescence-activated cell sorting (FACS) for $CD133^+$ ductal cells

● QUANTIFICATION AND STATISTICAL ANALYSIS

SUPPLEMENTAL INFORMATION

Supplemental information can be found online at https://doi.org/10.1016/j.isci.2024.109237.

ACKNOWLEDGMENTS

We thank services provided by the following research cores at the City of Hope: Analytical Flow Cytometry, Light Microscopy Digital Imaging, Integrative Genomics, Electron Microscopy, and Biostatistics. This work is supported, in part, by grants from the National Institutes of Health to H.T.K. (R01DK099734 and R56DK099734), the City of Hope Research Facilities (P30CA33572), and the Electron Microscopy core (P30CA0668). H.N.Z. is a recipient of a postdoctoral fellowship from the California Institute for Regenerative Medicine. Support from the Wanek Family Project for Type 1 Diabetes and from an anonymous donor, S.S., to H.T.K. is also gratefully acknowledged. We thank Dr. Hung-Ping (Ben) Shih for kindly providing the laminin antibody and for helpful discussions. The graphical abstract and some figure panels were prepared using BioRender.com.

AUTHOR CONTRIBUTIONS

Conceptualization, H.N.Z., J.C.Q., and H.T.K.; methodology, H.N.Z., J.C.Q., J.A.O., W.L., and I.G.; investigation, H.N.Z., J.C.Q., J.A.O., W.L., K.L., C.J.C.; validation, C.D., K.J., N.E., and C.J.C.; resources, E.M.; writing – original draft, H.N.Z. and H.T.K.; writing – reviewing and editing, all authors; funding acquisition, H.T.K.

DECLARATION OF INTERESTS

H.T.K. is an inventor of a patent no. 9,783,784, titled "Methods for establishing and improving the survival of a population of pancreatic progenitor or stem cells."

Received: June 19, 2023
Revised: December 22, 2023
Accepted: February 9, 2024
Published: February 15, 2024

REFERENCES

1. Bonner-Weir, S., Toschi, E., Inada, A., Reitz, P., Fonseca, S.Y., Aye, T., and Sharma, A. (2004). The pancreatic ductal epithelium serves as a potential pool of progenitor cells. Pediatr. Diabetes *5*, 16–22. https://doi.org/10.1111/j.1399-543X.2004.00075.x.
2. de Morree, A., and Rando, T.A. (2023). Regulation of adult stem cell quiescence and its functions in the maintenance of tissue integrity. Nat. Rev. Mol. Cell Biol. *24*, 334–354. https://doi.org/10.1038/s41580-022-00568-6.
3. Clevers, H., and Watt, F.M. (2018). Defining Adult Stem Cells by Function, not by Phenotype. Annu. Rev. Biochem. *87*, 1015–1027. https://doi.org/10.1146/annurev-biochem-062917-012341.
4. Mahla, R.S. (2016). Stem Cells Applications in Regenerative Medicine and Disease Therapeutics. Int. J. Cell Biol. *2016*, 6940283. https://doi.org/10.1155/2016/6940283.
5. Kulkarni, S., Posgai, A.L., Kusmartseva, I., Wasserfall, C.H., Atkinson, M.A., and Butler, A.E. (2022). Exocrine and Endocrine Inflammation Increases Cellular Replication in the Pancreatic Duct Compartment in Type 1 Diabetes. J. Endocr. Soc. *6*, bvac136. https://doi.org/10.1210/jendso/bvac136.
6. Moin, A.S.M., Butler, P.C., and Butler, A.E. (2017). Increased Proliferation of the Pancreatic Duct Gland Compartment in Type 1 Diabetes. J. Clin. Endocrinol. Metab. *102*, 200–209. https://doi.org/10.1210/jc.2016-3001.
7. Schludi, B., Moin, A.S.M., Montemurro, C., Gurlo, T., Matveyenko, A.V., Kirakossian, D., Dawson, D.W., Dry, S.M., Butler, P.C., and Butler, A.E. (2017). Islet inflammation and ductal proliferation may be linked to increased pancreatitis risk in type 2 diabetes. JCI insight *2*, e92282. https://doi.org/10.1172/jci.insight.92282.
8. Dirice, E., De Jesus, D.F., Kahraman, S., Basile, G., Ng, R.W., El Ouaamari, A., Teo, A.K.K., Bhatt, S., Hu, J., and Kulkarni, R.N. (2019). Human duct cells contribute to beta cell compensation in insulin resistance. JCI insight *4*, e99576. https://doi.org/10.1172/jci.insight.99576.
9. Georgakopoulos, N., Prior, N., Angres, B., Mastrogiovanni, G., Cagan, A., Harrison, D., Hindley, C.J., Arnes-Benito, R., Liau, S.S., Curd, A., et al. (2020). Long-term expansion, genomic stability and *in vivo* safety of adult human pancreas organoids. BMC Dev. Biol. *20*, 4. https://doi.org/10.1186/s12861-020-0209-5.

10. Loomans, C.J.M., Williams Giuliani, N., Balak, J., Ringnalda, F., van Gurp, L., Huch, M., Boj, S.F., Sato, T., Kester, L., de Sousa Lopes, S.M.C., et al. (2018). Expansion of Adult Human Pancreatic Tissue Yields Organoids Harboring Progenitor Cells with Endocrine Differentiation Potential. Stem Cell Rep. *10*, 712–724. https://doi.org/10.1016/j.stemcr.2018.02.005.
11. Qadir, M.M.F., Álvarez-Cubela, S., Klein, D., Lanzoni, G., García-Santana, C., Montalvo, A., Pláceres-Uray, F., Mazza, E.M.C., Ricordi, C., Inverardi, L.A., et al. (2018). P2RY1/ALK3-Expressing Cells within the Adult Human Exocrine Pancreas Are BMP-7 Expandable and Exhibit Progenitor-like Characteristics. Cell Rep. *22*, 2408–2420. https://doi.org/10.1016/j.celrep.2018.02.006.
12. Quijano, J.C., Wedeken, L., Ortiz, J.A., Zook, H.N., LeBon, J.M., Luo, A., Rawson, J., Tremblay, J.R., Mares, J.M., Lopez, K., et al. (2023). Methylcellulose colony assay and single-cell micro-manipulation reveal progenitor-like cells in adult human pancreatic ducts. Stem Cell Rep. *18*, 618–635. https://doi.org/10.1016/j.stemcr.2023.02.001.
13. Hughes, C.S., Postovit, L.M., and Lajoie, G.A. (2010). Matrigel: a complex protein mixture required for optimal growth of cell culture. Proteomics *10*, 1886–1890. https://doi.org/10.1002/pmic.200900758.
14. Borries, M., Barooji, Y.F., Yennek, S., Grapin-Botton, A., Berg-Sorensen, K., and Oddershede, L.B. (2020). Quantification of Visco-Elastic Properties of a Matrigel for Organoid Development as a Function of Polymer Concentration. Front. Phys *8*, 579168. https://doi.org/10.3389/fphy.2020.579168.
15. Perko, T., Markočič, E., Knez, Ž., and Škerget, M. (2011). Solubility and Diffusivity of CO2 in Natural Methyl Cellulose and Sodium Carboxymethyl Cellulose. J. Chem. Eng. Data *56*, 4040–4044. https://doi.org/10.1021/je200483p.
16. Jin, L., Feng, T., Zerda, R., Chen, C.C., Riggs, A.D., and Ku, H.T. (2014). *In vitro* multilineage differentiation and self-renewal of single pancreatic colony-forming cells from adult C57BL/6 mice. Stem Cells Dev. *23*, 899–909. https://doi.org/10.1089/scd.2013.0466.
17. Jin, L., Feng, T., Shih, H.P., Zerda, R., Luo, A., Hsu, J., Mahdavi, A., Sander, M., Tirrell, D.A., Riggs, A.D., and Ku, H.T. (2013). Colony-forming cells in the adult mouse pancreas are expandable in Matrigel and form endocrine/acinar colonies in laminin hydrogel. Proc. Natl. Acad. Sci. USA *110*, 3907–3912. https://doi.org/10.1073/pnas.1301889110.
18. Jin, L., Gao, D., Feng, T., Tremblay, J.R., Ghazalli, N., Luo, A., Rawson, J., Quijano, J.C., Chai, J., Wedeken, L., et al. (2016). Cells with surface expression of CD133highCD71low are enriched for tripotent colony-forming progenitor cells in the adult murine pancreas. Stem Cell Res. *16*, 40–53. https://doi.org/10.1016/j.scr.2015.11.015.
19. Scholzen, T., and Gerdes, J. (2000). The Ki-67 protein: from the known and the unknown. J. Cell. Physiol. *182*, 311–322. https://doi.org/10.1007/s00412-018-0659-8.
20. Krah, N.M., De La O, J.P., Swift, G.H., Hoang, C.Q., Willet, S.G., Chen Pan, F., Cash, G.M., Bronner, M.P., Wright, C.V., MacDonald, R.J., and Murtaugh, L.C. (2015). The acinar differentiation determinant PTF1A inhibits initiation of pancreatic ductal adenocarcinoma. Elife *4*, e07125. https://doi.org/10.7554/eLife.07125.
21. Backx, E., Wauters, E., Baldan, J., Van Bulck, M., Michiels, E., Heremans, Y., De Paep, D.L., Kurokawa, M., Goyama, S., Bouwens, L., et al. (2021). MECOM permits pancreatic acinar cell dedifferentiation avoiding cell death under stress conditions. Cell Death Differ. *28*, 2601–2615. https://doi.org/10.1038/s41418-021-00771-6.
22. Baldan, J., Houbracken, I., Rooman, I., and Bouwens, L. (2019). Adult human pancreatic acinar cells dedifferentiate into an embryonic progenitor-like state in 3D suspension culture. Sci. Rep. *9*, 4040. https://doi.org/10.1038/s41598-019-40481-1.
23. Kaur, S., Kumar, S., Momi, N., Sasson, A.R., and Batra, S.K. (2013). Mucins in pancreatic cancer and its microenvironment. Nat. Rev. Gastroenterol. Hepatol. *10*, 607–620. https://doi.org/10.1038/nrgastro.2013.120.
24. Segerstolpe, Å., Palasantza, A., Eliasson, P., Andersson, E.M., Andréasson, A.C., Sun, X., Picelli, S., Sabirsh, A., Clausen, M., Bjursell, M.K., et al. (2016). Single-Cell Transcriptome Profiling of Human Pancreatic Islets in Health and Type 2 Diabetes. Cell Metab. *24*, 593–607. https://doi.org/10.1016/j.cmet.2016.08.020.
25. Co, J.Y., Margalef-Català, M., Li, X., Mah, A.T., Kuo, C.J., Monack, D.M., and Amieva, M.R. (2019). Controlling Epithelial Polarity: A Human Enteroid Model for Host-Pathogen Interactions. Cell Rep. *26*, 2509–2520.e4. https://doi.org/10.1016/j.celrep.2019.01.108.
26. Wijesekara, P., Yadav, P., Perkins, L.A., Stolz, D.B., Franks, J.M., Watkins, S.C., Reinoso Jacome, E., Brody, S.L., Horani, A., Xu, J., et al. (2022). Engineering rotating apical-out airway organoid for assessing respiratory cilia motility. iScience *25*, 104730. https://doi.org/10.1016/j.isci.2022.104730.
27. Manninen, A. (2015). Epithelial polarity – Generating and integrating signals from the ECM with integrins. Exp. Cell Res. *334*, 337–349. https://doi.org/10.1016/j.yexcr.2015.01.003.
28. Soofi, S.S., Last, J.A., Liliensiek, S.J., Nealey, P.F., and Murphy, C.J. (2009). The elastic modulus of Matrigel as determined by atomic force microscopy. J. Struct. Biol. *167*, 216–219. https://doi.org/10.1016/j.jsb.2009.05.005.
29. Jimenez-Caliani, A.J., Pillich, R., Yang, W., Diaferia, G.R., Meda, P., Crisa, L., and Cirulli, V. (2017). alphaE-Catenin Is a Positive Regulator of Pancreatic Islet Cell Lineage Differentiation. Cell Rep. *20*, 1295–1306. https://doi.org/10.1016/j.celrep.2017.07.035.
30. Jorgens, D.M., Inman, J.L., Wojcik, M., Robertson, C., Palsdottir, H., Tsai, W.T., Huang, H., Bruni-Cardoso, A., López, C.S., Bissell, M.J., et al. (2017). Deep nuclear invaginations are linked to cytoskeletal filaments - integrated bioimaging of epithelial cells in 3D culture. J. Cell Sci. *130*, 177–189. https://doi.org/10.1242/jcs.190967.
31. Jiang, F.X., Naselli, G., and Harrison, L.C. (2002). Distinct distribution of laminin and its integrin receptors in the pancreas. J. Histochem. Cytochem. *50*, 1625–1632. https://doi.org/10.1177/002215540205001206.
32. Walker, C., Mojares, E., and Del Río Hernández, A. (2018). Role of Extracellular Matrix in Development and Cancer Progression. Int. J. Mol. Sci. *19*, 3028. https://doi.org/10.3390/ijms19103028.
33. Pucci, B., Kasten, M., and Giordano, A. (2000). Cell cycle and apoptosis. Neoplasia *2*, 291–299. https://doi.org/10.1038/sj.neo.7900101.
34. Taddei, M.L., Giannoni, E., Fiaschi, T., and Chiarugi, P. (2012). Anoikis: an emerging hallmark in health and diseases. J. Pathol. *226*, 380–393. https://doi.org/10.1002/path.3000.
35. Eskandari, E., and Eaves, C.J. (2022). Paradoxical roles of caspase-3 in regulating cell survival, proliferation, and tumorigenesis. J. Cell Biol. *221*, e202201159. https://doi.org/10.1083/jcb.202201159.
36. Porter, A.G., and Jänicke, R.U. (1999). Emerging roles of caspase-3 in apoptosis. Cell Death Differ. *6*, 99–104. https://doi.org/10.1038/sj.cdd.4400476.
37. Vander Heiden, M.G., Cantley, L.C., and Thompson, C.B. (2009). Understanding the Warburg effect: the metabolic requirements of cell proliferation. Science *324*, 1029–1033. https://doi.org/10.1126/science.1160809.
38. Khoshnoodi, J., Pedchenko, V., and Hudson, B.G. (2008). Mammalian collagen IV. Microsc. Res. Tech. *71*, 357–370. https://doi.org/10.1002/jemt.20564.
39. Zeltz, C., and Gullberg, D. (2016). The integrin–collagen connection – a glue for tissue repair? J. Cell Sci. *129*, 653–664. https://doi.org/10.1242/jcs.180992.
40. Lusche, D.F., Klemme, M.R., Soll, B.A., Reis, R.J., Forrest, C.C., Nop, T.S., Wessels, D.J., Berger, B., Glover, R., and Soll, D.R. (2019). Integrin α-3 ß-1's central role in breast cancer, melanoma and glioblastoma cell aggregation revealed by antibodies with blocking activity. mAbs *11*, 691–708. https://doi.org/10.1080/19420862.2019.1583987.
41. Öhlund, D., Franklin, O., Lundberg, E., Lundin, C., and Sund, M. (2013). Type IV collagen stimulates pancreatic cancer cell proliferation, migration, and inhibits apoptosis through an autocrine loop. BMC Cancer *13*, 154. https://doi.org/10.1186/1471-2407-13-154.
42. Hamilton, N.J.I., Lee, D.D.H., Gowers, K.H.C., Butler, C.R., Maughan, E.F., Jevans, B., Orr, J.C., McCann, C.J., Burns, A.J., MacNeil, S., et al. (2020). Bioengineered airway epithelial grafts with mucociliary function based on collagen IV- and laminin-containing extracellular matrix scaffolds. Eur. Respir. J. *55*, 1901200. https://doi.org/10.1183/13993003.01200-2019.
43. Wu, D., Witt, R.L., Harrington, D.A., and Farach-Carson, M.C. (2019). Dynamic Assembly of Human Salivary Stem/Progenitor Microstructures Requires Coordinated alpha(1)beta(1) Integrin-Mediated Motility. Front. Cell Dev. Biol. *7*, 224. https://doi.org/10.3389/fcell.2019.00224.
44. Gjorevski, N., Sachs, N., Manfrin, A., Giger, S., Bragina, M.E., Ordóñez-Morán, P., Clevers, H., and Lutolf, M.P. (2016). Designer matrices for intestinal stem cell and organoid culture. Nature *539*, 560–564. https://doi.org/10.1038/nature20168.
45. Capeling, M.M., Huang, S., Childs, C.J., Wu, J.H., Tsai, Y.H., Wu, A., Garg, N., Holloway, E.M., Sundaram, N., Bouffi, C., et al. (2022). Suspension culture promotes serosal mesothelial development in human intestinal organoids. Cell Rep. *38*, 110379. https://doi.org/10.1016/j.celrep.2022.110379.
46. Garnier, D., Li, R., Delbos, F., Fourrier, A., Collet, C., Guguen-Guillouzo, C., Chesne, C., and Nguyen, T.H. (2018). Expansion of human primary hepatocytes *in vitro* through their

amplification as liver progenitors in a 3D organoid system. https://doi.org/10.1038/s41598-018-26584-1.

47. Hirokawa, Y., Clarke, J., Palmieri, M., Tan, T., Mouradov, D., Li, S., Lin, C., Li, F., Luo, H., Wu, K., et al. (2021). Low-viscosity matrix suspension culture enables scalable analysis of patient-derived organoids and tumoroids from the large intestine. Commun. Biol. *4*, 1067. https://doi.org/10.1038/s42003-021-02607-y.
48. Sahu, S., Albaugh, M.E., Martin, B.K., Patel, N.L., Riffle, L., Mackem, S., Kalen, J.D., and Sharan, S.K. (2022). Growth factor dependency in mammary organoids regulates ductal morphogenesis during organ regeneration. https://doi.org/10.1038/s41598-022-11224-6.
49. Wrenn, E.D., Moore, B.M., Greenwood, E., McBirney, M., and Cheung, K.J. (2020). Optimal, Large-Scale Propagation of Mouse Mammary Tumor Organoids. J. Mammary Gland Biol. Neoplasia *25*, 337–350. https://doi.org/10.1007/s10911-020-09464-1.
50. Kakni, P., López-Iglesias, C., Truckenmüller, R., Habibović, P., and Giselbrecht, S. (2022). Reversing Epithelial Polarity in Pluripotent Stem Cell-Derived Intestinal Organoids. Front. Bioeng. Biotechnol. *10*, 879024. https://doi.org/10.3389/fbioe.2022.879024.
51. Bates, R.C., Buret, A., van Helden, D.F., Horton, M.A., and Burns, G.F. (1994). Apoptosis induced by inhibition of intercellular contact. J. Cell Biol. *125*, 403–415. https://doi.org/10.1083/jcb.125.2.403.
52. Bretland, A.J., Lawry, J., and Sharrard, R.M. (2001). A study of death by anoikis in cultured epithelial cells. Cell Prolif. *34*, 199–210. https://doi.org/10.1046/j.1365-2184.2001.00198.x.
53. Frisch, S.M., and Francis, H. (1994). Disruption of epithelial cell-matrix interactions induces apoptosis. J. Cell Biol. *124*, 619–626. https://doi.org/10.1083/jcb.124.4.619.
54. Moreno-Layseca, P., and Streuli, C.H. (2014). Signalling pathways linking integrins with cell cycle progression. Matrix Biol. *34*, 144–153. https://doi.org/10.1016/j.matbio.2013.10.011.
55. Pozzi, A., Wary, K.K., Giancotti, F.G., and Gardner, H.A. (1998). Integrin alpha1beta1 mediates a unique collagen-dependent proliferation pathway *in vivo*. J. Cell Biol. *142*, 587–594. https://doi.org/10.1083/jcb.142.2.587.
56. Kim, E.J.Y., Sorokin, L., and Hiiragi, T. (2022). ECM-integrin signalling instructs cellular position sensing to pattern the early mouse embryo. Development *149*. https://doi.org/10.1242/dev.200140.
57. Walma, D.A.C., and Yamada, K.M. (2020). The extracellular matrix in development. Development *147*. https://doi.org/10.1242/dev.175596.
58. Means, A.L. (2013). Pancreatic stellate cells: small cells with a big role in tissue homeostasis. Lab. Invest. *93*, 4–7. https://doi.org/10.1038/labinvest.2012.161.
59. Kaido, T., Yebra, M., Cirulli, V., and Montgomery, A.M. (2004). Regulation of human beta-cell adhesion, motility, and insulin secretion by collagen IV and its receptor alpha1beta1. J. Biol. Chem. *279*, 53762–53769. https://doi.org/10.1074/jbc.M411202200.
60. Riopel, M., and Wang, R. (2014). Collagen matrix support of pancreatic islet survival and function. Front. Biosci. *19*, 77–90. https://doi.org/10.2741/4196.
61. Rovira, M., Scott, S.G., Liss, A.S., Jensen, J., Thayer, S.P., and Leach, S.D. (2010). Isolation and characterization of centroacinar/terminal ductal progenitor cells in adult mouse pancreas. Proc. Natl. Acad. Sci. USA *107*, 75–80. https://doi.org/10.1073/pnas.0912589107.
62. Seaberg, R.M., Smukler, S.R., Kieffer, T.J., Enikolopov, G., Asghar, Z., Wheeler, M.B., Korbutt, G., and van der Kooy, D. (2004). Clonal identification of multipotent precursors from adult mouse pancreas that generate neural and pancreatic lineages. Nat. Biotechnol. *22*, 1115–1124. https://doi.org/10.1038/nbt1004.
63. Smukler, S.R., Arntfield, M.E., Razavi, R., Bikopoulos, G., Karpowicz, P., Seaberg, R., Dai, F., Lee, S., Ahrens, R., Fraser, P.E., et al. (2011). The adult mouse and human pancreas contain rare multipotent stem cells that express insulin. Cell Stem Cell *8*, 281–293. https://doi.org/10.1016/j.stem.2011.01.015.
64. Tang, X., Kusmartseva, I., Kulkarni, S., Posgai, A., Speier, S., Schatz, D.A., Haller, M.J., Campbell-Thompson, M., Wasserfall, C.H., Roep, B.O., et al. (2021). Image-Based Machine Learning Algorithms for Disease Characterization in the Human Type 1 Diabetes Pancreas. Am. J. Pathol. *191*, 454–462. https://doi.org/10.1016/j.ajpath.2020.11.010.
65. Grasso, D., Ropolo, A., Lo Ré, A., Boggio, V., Molejón, M.I., Iovanna, J.L., Gonzalez, C.D., Urrutia, R., and Vaccaro, M.I. (2011). Zymophagy, a novel selective autophagy pathway mediated by VMP1-USP9x-p62, prevents pancreatic cell death. J. Biol. Chem. *286*, 8308–8324. https://doi.org/10.1074/jbc.M110.197301.
66. Pagliuca, F.W., Millman, J.R., Gürtler, M., Segel, M., Van Dervort, A., Ryu, J.H., Peterson, Q.P., Greiner, D., and Melton, D.A. (2014). Generation of functional human pancreatic beta cells *in vitro*. Cell *159*, 428–439. https://doi.org/10.1016/j.cell.2014.09.040.
67. Russ, H.A., Parent, A.V., Ringler, J.J., Hennings, T.G., Nair, G.G., Shveygert, M., Guo, T., Puri, S., Haataja, L., Cirulli, V., et al. (2015). Controlled induction of human pancreatic progenitors produces functional beta-like cells *in vitro*. EMBO J. *34*, 1759–1772. https://doi.org/10.15252/embj.201591058.
68. Kozlowski, M.T., Crook, C.J., and Ku, H.T. (2021). Towards organoid culture without Matrigel. Commun. Biol. *4*, 1387. https://doi.org/10.1038/s42003-021-02910-8.
69. Qi, M., Valiente, L., McFadden, B., Omori, K., Bilbao, S., Juan, J., Rawson, J., Scott, S., Ferreri, K., Mullen, Y., et al. (2015). The Choice of Enzyme for Human Pancreas Digestion is a Critical Factor for Increasing the Success of Islet Isolation. Transplant. Direct *1*, e14. https://doi.org/10.1097/TXD.0000000000000522.
70. Bolger, A.M., Lohse, M., and Usadel, B. (2014). Trimmomatic: a flexible trimmer for Illumina sequence data. Bioinformatics *30*, 2114–2120. https://doi.org/10.1093/bioinformatics/btu170.
71. Chen, S., Zhou, Y., Chen, Y., and Gu, J. (2018). fastp: an ultra-fast all-in-one FASTQ preprocessor. Bioinformatics *34*, i884–i890. https://doi.org/10.1093/bioinformatics/bty560.
72. Dobin, A., Davis, C.A., Schlesinger, F., Drenkow, J., Zaleski, C., Jha, S., Batut, P., Chaisson, M., and Gingeras, T.R. (2013). STAR: ultrafast universal RNA-seq aligner. Bioinformatics *29*, 15–21. https://doi.org/10.1093/bioinformatics/bts635.
73. Anders, S., and Huber, W. (2010). Differential expression analysis for sequence count data. Genome Biol. *11*, R106. https://doi.org/10.1186/gb-2010-11-10-r106.
74. Robinson, M.D., McCarthy, D.J., and Smyth, G.K. (2010). edgeR: a Bioconductor package for differential expression analysis of digital gene expression data. Bioinformatics *26*, 139–140. https://doi.org/10.1093/bioinformatics/btp616.
75. Mootha, V.K., Lindgren, C.M., Eriksson, K.F., Subramanian, A., Sihag, S., Lehar, J., Puigserver, P., Carlsson, E., Ridderstråle, M., Laurila, E., et al. (2003). PGC-1alpha-responsive genes involved in oxidative phosphorylation are coordinately downregulated in human diabetes. Nat. Genet. *34*, 267–273. https://doi.org/10.1038/ng1180.
76. Subramanian, A., Tamayo, P., Mootha, V.K., Mukherjee, S., Ebert, B.L., Gillette, M.A., Paulovich, A., Pomeroy, S.L., Golub, T.R., Lander, E.S., and Mesirov, J.P. (2005). Gene set enrichment analysis: a knowledge-based approach for interpreting genome-wide expression profiles. Proc. Natl. Acad. Sci. USA *102*, 15545–15550. https://doi.org/10.1073/pnas.0506580102.

STAR★METHODS

KEY RESOURCES TABLE

REAGENT or RESOURCE	SOURCE	IDENTIFIER
Antibodies		
Armenian Hamster anti-Mucin 1	Neomarkers/Thermo Fisher	Cat# 1630-PI; RRID: AB_11000874
Guinea pig anti-PDX1	Abcam	Cat# ab47308; RRID: AB_777178
Goat anti-CDH1	R&D Systems	Cat# AF748; RRID: AB_355568
Rabbit anti-KRT19	Abcam	Cat# ab52625; RRID: AB_2281020
Goat anti-NKX6.1	Novus/R&D Systems	Cat# AF5857; RRID: AB_1857045
Rabbit anti-SOX9	Chemicon/Millipore-Sigma	Cat# AB5535; RRID: AB_2239761
Mouse anti-KI67	BD Biosciences	Cat# 550609; RRID: AB_393778
Rat anti-KI67, FITC conjugated	Thermo Fisher	Cat# 11-5698-82; RRID: AB_11151330
Rabbit anti-CC3	Cell Signaling	Cat# 9661S; RRID: AB_2341188
Mouse anti-CD133, biotin conjugated	Miltenyi Biotec	Cat# 130-113-747; RRID: AB_2726286
Mouse anti-CD49a (Integrin α1)	Novus Biologicals	Cat# NBP2-29757; RRID: AB_2938701
Mouse anti-CD29 (Integrin β1)	R&D Systems	Cat# MAB17781; RRID: AB_2129940
Mouse IgG1	R&D Systems	Cat# MAB002; RRID: AB_357344
Mouse IgG2A	R&D Systems	Cat# MAB0031; RRID: AB_471244
Streptavidin-APC	Miltenyi Biotec	Cat# 130-106-792; RRID: AB_2661578
Donkey anti-Armenian Hamster AF647	Jackson ImmunoResearch	Cat# 127-605-160; RRID: AB_2339001
Donkey anti-Goat AF488	Jackson ImmunoResearch	Cat# 705-545-147; RRID: AB_2336933
Donkey anti-Goat AF647	Jackson ImmunoResearch	Cat# 705-605-147; RRID: AB_2340437
Donkey anti-Guinea Pig AF647	Jackson ImmunoResearch	Cat# 706-606-148; RRID: AB_2340477
Donkey anti-Mouse FITC	Jackson ImmunoResearch	Cat# 715-095-151; RRID: AB_2335588
Donkey anti-Rabbit AF488	Jackson ImmunoResearch	Cat# 711-546-152; RRID: AB_2340619
Donkey anti-Rabbit Cy3	Jackson ImmunoResearch	Cat# 711-165-152; RRID: AB_2307443
Biological samples		
Islet-depleted adult human pancreatic tissue	Southern California Islet Cell Resource Center at City of Hope	https://iidp.coh.org/Centers
Chemicals, peptides, and recombinant proteins		
Penicillin-Streptomycin	Gibco	Cat# 15140-122
Cell Recovery Solution	Corning	Cat# 354253
KnockOut Serum Replacement	Thermo Fisher	Cat# 10828-028
Nicotinamide	Sigma-Aldrich	Cat# N0636
Exendin 4	Sigma-Aldrich	Cat# E7144
SB-202190	Sigma-Aldrich	Cat# S7067
Gastrin II Sulfated	Sigma-Aldrich	Cat# G1260
Recombinant mouse R-Spondin1 (RSPO1)	R&D Systems	Cat# 3474-RS
Recombinant human vascular endothelial growth factor (VEGF)	R&D Systems	Cat# 293-VE
Recombinant human epidermal growth factor (EGF)	R&D Systems	Cat# 236-EG
Recombinant mouse Noggin	R&D Systems	Cat# 1967-NG
A83-01	Tocris	Cat# 2939
Y-27632 (Ri)	R&D Systems	Cat# 1254/10
Collagenase B	Sigma-Aldrich	Cat# 11088831001

(*Continued on next page*)

Continued

REAGENT or RESOURCE	SOURCE	IDENTIFIER
Bovine Desoxyribonuclease (DNase) I	VWR	Cat# 80510-412
Liberase™ TH	Sigma-Aldrich	Cat# 05 401 151 001
CTS™ TrypLE™ Select Enzyme	Thermo Fisher	Cat# A1285901
4′,6-diamidino-2-phenylindole (DAPI)	Invitrogen	Cat# D3571
Hoechst 33342	Abcam	Cat# ab228551
5-ethynyl-2′-deoxyuridine (EdU)	Abcam	Cat# ab146186
VECTASHIELD® Vibrance Antifade Mounting Medium	Vector Laboratories	Cat# H-1700-10
Vector TrueVIEW Autofluorescence Quenching Kit	Vector Laboratories	Cat# SP-8400-15
DMEM (Dulbecco's Modified Eagle's Medium)/Hams F-12 50/50 Mix	Corning	Cat# 10-092-CV
Paraformaldehyde solution (4%) in PBS	Santa Cruz	Cat# sc-281692; CAS 30525-89-4
Critical commercial assays		
RNeasy Microkit	Qiagen	Cat #74004
ECM Select® Array Kit Ultra-36	Advanced Biomatrix	Cat# 5170
CellsDirect™ One-Step qRT-PCR Kit	Thermo Fisher	Cat# 11753100
TaqMan™ Universal PCR Master Mix	Applied Biosystems	Cat# 4304437
QuantiTect Reverse Transcription Kit	Qiagen	Cat# 205313
Chromium Next GEM Single Cell 3′ Library Construction Kit v3	10X Genomics	Cat# PN-1000092
Click-iT™ EdU Alexa Fluor™ 488 Imaging Kit	Thermo Fisher	Cat# C10337
Deposited data		
Raw and analyzed scRNA-seq data of suspension cells	This paper	GEO: GSE233785 (or GSE233786)
Raw and analyzed scRNA-seq data of human exocrine tissue	Quijano et al.	GEO: GSE153834
Raw and analyzed bulk mRNA-seq data	This paper	GEO: GSE233344 (or GSE233786)
Oligonucleotides		
Taqman probes used in conventional and microfluidic qRT-PCR, see Table S4.	This paper	N/A
Software and algorithms		
ImageJ	Version 1.53e	https://imagej.nih.gov/ij/
FlowJo	Version 10.8.1	https://www.flowjo.com/
GraphPad Prism	Version 9.5.1	https://www.graphpad.com/scientific-software/prism/
CellRanger	Version 3.0.1	https://support.10xgenomics.com/single-cell-gene-expression/software/pipelines/latest/what-is-cell-ranger
R	Version 4.1.0	https://www.r-project.org/
Seurat (R package)	Version 4.3.0	https://satijalab.org/seurat/
Adobe Photoshop	Version 24.4.1	https://www.adobe.com/products/photoshop.html
Adobe Illustrator	Version 27.5	https://www.adobe.com/products/illustrator.html
Fluidigm Real-Time PCR Analysis	Version 4.1.3	https://www.standardbio.com/
Zen Blue	Version 2.5	https://www.zeiss.com/microscopy/en/products/software/zeiss-zen.html
Other		
Matrigel® Growth Factor Reduced (GFR) Basement Membrane Matrix, Phenol Red-free, LDEV-free	Corning	Cat# 356231
Methylcellulose, 1500 cPs	Shin-Etsu	CAS 9004-67-5

(*Continued on next page*)

Continued

REAGENT or RESOURCE	SOURCE	IDENTIFIER
Collagen IV	Advanced Biomatrix	Cat# 5022
Vitronectin	Advanced Biomatrix	Cat# 5051
Collagen VI	Abcam	Cat# ab7538

RESOURCE AVAILABILITY

Lead contact

Further information and requests for resources and reagents should be directed to and will be fulfilled by the Lead Contact, Hsun Teresa Ku (hku@coh.org).

Materials availability

This study did not generate new unique reagents.

Data and code availability

- The raw and analyzed single-cell RNA-sequencing and bulk mRNA-sequencing data generated in this paper were deposited in the Gene Expression Omnibus (GEO, https://www.ncbi.nlm.nih.gov/geo/), and are publicly available as of the date of publication. Accession numbers are listed in the key resources table.
- This paper does not report original code.
- Any additional information required to reanalyze the data reported in this paper is available from the lead contact upon request.

EXPERIMENTAL MODEL AND STUDY PARTICIPANT DETAILS

Donated pancreata were procured and shipped to the Southern California Islet Cell Resource (SC-ICR) Center at City of Hope for isolation of islets.[69] All seventeen pancreatic tissues used in this study had consent for research from close relatives of the donors. After islet removal, de-identified human pancreas exocrine tissues were distributed by the SC-ICR and we processed the exocrine tissues into single-cell suspension within 5 days as described below.

METHOD DETAILS

Primary tissue single-cell suspension preparation

Primary exocrine tissue was rinsed once in cold PBS and resuspended in Dulbecco's phosphate-buffered saline (PBS) containing 0.1% bovine serum albumin (BSA), collagenase B (2-4 mg/mL) (Roche, Mannheim, Germany), and DNase I (2,000 U/mL) (Calbiochem, Darmstadt, Germany). The solution was incubated at 37°C for 30 min, during which the tissue was gently disrupted every 5-10 min using a 16 ½" G syringe needle. Cells were washed twice in dPBS+BSA+DNase I and filtered sequentially through 100 μm and 40 μm nylon meshes (BD Biosciences, San Jose, USA) to yield a single-cell suspension before cryopreservation or culture. Donor characteristics are described in Table S1.

Cryopreservation of primary tissue

Dissociated single-cell suspensions were counted, pelleted, gently resuspended in Cryostor (BioLife Solutions, Bothell, USA), and frozen using a CryoMed™ Controlled-Rate Freezer (Thermo Scientific, Waltham, USA). After cryopreservation, vials were transferred to a liquid nitrogen tank for long-term storage. To thaw, frozen vials were placed in a 37°C water bath for 2 minutes, gently transferred to a 15 mL conical tube, and washed once with warm PBS supplemented with 0.1% BSA. Pellets were gently resuspended in either warm Dulbecco's Modified Eagle's Medium/Hams F-12 50/50 Mix (DMEM/F12)+Penicillin-Streptavidin (PS) or suspension culture medium.

3-Dimensional (3D) colony assay

Dissociated single-cell suspensions from cryopreservation or suspension culture were seeded at a density between 500 and 5,000 cells in 0.5 mL per well.[12] The culture medium for adult human cells contained DMEM/F12, KnockOut Serum Replacement, PS, methylcellulose (1% w/v), Matrigel (5% v/v), and exogenous growth factors and small molecules. For the 9-factor (9F) medium, nicotinamide, Noggin, epidermal growth factor (EGF), A83-01, SB-202190, Rspondin-1 (RSPO1), exendin-4, vascular endothelial growth factor-A (VEGF), and gastrin II (sulfated) were used (see key resources table and Table S2). The 6-factor (6F) medium omitted exendin-4, VEGF, and SB202190. Cells were plated in 24-well ultra-low protein-binding plates (Corning, New York, USA) and incubated in a humidified 5% CO_2 atmosphere at 37°C. Delayed addition of Y-27632 (Rock inhibitor, Ri) was accomplished by distributing 50 μL of vehicle or Ri solution (diluted in DMEM/F12+PS) per well on top of the medium and gently rocking the plate for 30 seconds to mix. Otherwise, vehicle or Ri was directly mixed into the culture medium with the other growth factors and small molecules. Analysis of colonies was done 3 weeks post-plating. Colonies were imaged, counted, and collected for analysis. Colony-forming efficiency was calculated by dividing the number of colonies formed by the total number

of cells plated per well. Colonies were imaged and diameters were measured using Infinity Analyze software (Lumenera Corporation, Ottawa, CAN).

Self-renewal colony assay

Cells were plated into the colony assay in a primary culture. Three weeks later, colonies were collected, pooled, and washed in warm PBS+0.1% BSA. Colonies were dissociated into single cells by incubation with 0.25% trypsin-ethylenediaminetetraacetic acid (EDTA) at 37°C for 5 min, followed by gentle pipetting. Single cells were counted and diluted, and a fraction of the cells were re-plated into a new 24-well plate at a concentration of up to 5,000 cells in 0.5 mL per well (secondary culture). This process was repeated once more (tertiary culture). The final total number of progenitors was calculated by multiplying the previous dilution factor(s) with the number of colonies per well in the culture.

3D suspension culture

Dissociated single-cell suspensions were cultured at a density of 400,000 cells in 0.5 mL per well. The culture medium contained DMEM/F12, KnockOut Serum Replacement, PS, nicotinamide, Noggin, EGF, A83-01, RSPO1, and gastrin. Cells were plated in 24-well ultra-low binding plates (Corning) and incubated in a humidified 5% CO_2 atmosphere at 37°C. Ri was added to the culture medium for initial overnight incubation (up to 16 h). To change the medium, culture day (D) 1 cells were collected, pooled, and washed in warm DMEM/F12+0.1% BSA+PS. Cells were re-suspended in fresh suspension medium without Ri. On D4, cells were collected, pooled, and centrifuged at 100 x g for 1 min. 90% of the medium was aspirated and replaced with fresh suspension medium.

For ECM protein addition experiments, suspension culture medium was prepared and incubated on ice for at least 5 min. Next, ECM proteins were added at appropriate dilutions using cold pipette tips and mixed by gentle pipetting. Culture medium was brought to room temperature before it was added to cells. To prepare the cells, D1 cells were collected, pooled, and washed as above. Live cells were enriched using Histopaque-1077 (Sigma-Aldrich, St. Louis, USA). This was done by gently layering up to $5x10^6$ D1 cells re-suspended in 3 mL DMEM/F12+0.1%BSA+PS atop an equal volume of room-temperature Histopaque-1077. Then, cells were centrifuged at 400 x g for 15 min with acceleration values set at 1 and deceleration values set at 0 (Sorvall ST40R centrifuge). Cells at the interphase layer were collected in <2 mL volume, washed with DMEM/F12+0.1%BSA+PS two times, counted, and re-suspended with room-temperature suspension culture medium supplemented with ECM proteins. Cells were plated into ultra-low binding plates as follows: 150,000 cells per 0.5 mL per well (24-well plate), 15,000 cells in 0.1 mL per well (96-well plate; Thermo Fisher), or between 5,000 and 7,500 cells in 0.05 mL per well (384-well plate; VWR International, Radnor, USA). Cells were then incubated in a humidified 5% CO_2 atmosphere at 37°C.

Suspension cultured spheroids or cysts were dissociated for analysis or replating by collecting replicates into individual Eppendorf or 15 mL Falcon tubes, washing with warm DMEM/F12+0.1%BSA+PS, and then sequentially incubating with Liberase™ TH (0.56 U/mL; Sigma-Aldrich) and TrypLE (100%; Thermo Fisher) for up to 10 min each. Gentle pipetting was used during each incubation step to mechanically disperse the spheroids. Fetal bovine serum (FBS) was used to stop the TrypLE enzymatic reaction. Cells were washed at least twice during each step using warm DMEM/F12+0.1%BSA+PS and were centrifuged at 400xg for 5 min. Single cells were resuspended in DMEM/F12+PS, counted, and used for downstream applications.

Microfluidic and conventional quantitative (q)RT-PCR

For microfluidic qRT-PCR,[12] individual micro-manipulated colonies or suspension cells were collected in 10 μL of reaction buffer (CellsDirect One-Step qRT-PCR Kit, Invitrogen, Carlsbad, USA) and pre-amplified (14 cycles) according to the manufacturer's instructions (Fluidigm-Biomark, San Francisco, USA; Invitrogen). Pre-amplified cDNA was loaded onto a 48.48 Dynamic Array system using the NanoFlex integrated fluidic circuit (IFC) controller (Fluidigm). Threshold cycle (Ct) was used to measure fluorescence intensity. Ct values were determined using BioMark PCR analysis software (Fluidigm) and expressed either as a heat map or relative expression (delta Ct) of the gene of interest compared to the internal control gene. *B2 microglobulin* (*B2M*) was used as the internal control to calculate relative expression. All reactions were performed with negative (water) and positive (cDNA from adult human islet cells) controls. Taqman probes (Life Technologies, Carlsbad, USA) and their catalog numbers are listed in Table S3.

For conventional qRT-PCR, total RNA extraction and reverse transcription was performed according to manufacturer's instructions using the RNeasy Micro Kit (Qiagen, Valencia, CA). *β-actin* was used as the internal control for normalization. Two or three technical replicates were used in all PCR runs.

Immunofluorescence staining

For frozen embedding of suspension-cultured samples, cells were pooled, washed once with PBS+0.1% BSA+PS, and then washed once with PBS. Samples cultured with 5% Matrigel and their controls were incubated with Cell Recovery Solution (Corning) for 30 min in 4°C. All samples were then washed once more with PBS. Next, samples were fixed in 4% paraformaldehyde at 4°C overnight, then cryoprotected in 30% sucrose with PBS at 4°C overnight. Samples were then embedded in Optimal Cutting Temperature compound (23-730-571, Fisher Scientific) and frozen into blocks. Samples were cut into 10 μm thicknesses and saved at -80°C until staining.

Frozen sections were thawed at room temperature. After washing twice in PBS for 10 min, some samples underwent antigen retrieval for 40 min in 1x sodium citrate buffer (pH 6.0; Electron Microscopy Sciences, Hatfield) using the IHC-TekTM Epitope Retrieval Steamer Set

(IHC World LLC, Ellicott City). After washing and/or antigen retrieval, samples were blocked for 1 h at room temperature with buffer containing 5-10% donkey serum, 0.1% Triton X-100, and 1x PowerBlocker (Biogenex, Fremont). Slides were then incubated with primary antibodies overnight at 4°C, washed thrice with PBS and 0.1% Triton X-100, and incubated with donkey-raised secondary antibodies conjugated to Cy3, Cy5, AlexaFluor488, or AlexaFluor647 (Jackson ImmunoResearch, West Grove, USA) for 2 h at room temperature. Autofluorescence was minimized using TrueView kit (SP-8400-15, Vector Laboratories, Newark, USA) followed by 10 min incubation with 4′,6-diamidine-2′-phenylindole dihydrochloride (DAPI) to stain nuclei. Vectashield vibrance antifade mounting medium (H-1700, Vector Laboratories) was used to mount coverslips for imaging. For list of antibodies, see key resources table and Table S4.

Images were captured within three days of mounting using a Zeiss LSM880 with Airyscan, Zeiss Axio-Observer-Z1 with Apotome, or Zeiss Axio-Cam506. Figures were prepared using LSM Image Browser software (Carl Zeiss, Germany), Adobe Photoshop, and Adobe Illustrator. Quantification of images was performed using Adobe Photoshop by two or more investigators and at least ten unique images were used for each condition.

Preparation of samples for single-cell RNA sequencing

Exocrine tissue was dissociated into single cells, counted, and resuspended in suspension culture medium with Ri ("fresh"). On D1 and D4, medium was refreshed without Ri, as indicated above. In parallel, the same protocol was followed for cryopreserved ("cryo") samples. On D3 and D7 of each culture, fresh and cryo spheroids were dispersed as indicated above using Liberase™ TH and TrypLE. Viability measurements were performed manually with a hemocytometer and using a BioRad cell counter. An estimated 2,672 cells from fresh D3, 2,414 cells from fresh D7, 2,745 cells from cryo D3, and 2,729 cells from cryo D7 were captured on a 10xGenomics Chromium Controller using a 10X V3 Single Cell 3′ Solution kit (10xGenomics, Chromium Single Cell 3′ Reagent kit V3, PN-1000092). All protocols were performed following the manufacturer's instructions. Final sequencing libraries were analyzed on a High Sensitivity DNA Chip (5067-4626, Agilent Technologies, Santa Clara, USA). The library concentration was determined with a Qubit High Sensitivity DNA Assay Kit (Q32854, Thermo Fisher). The libraries were sequenced with the paired-end setting of 28 cycles of read (R) 1, 101 cycles of R2, and 8 cycles of index reads on Illumina NovaSeq 6000 platform, with sequencing depth of ~0.1 million reads per cell.

Computational analysis of single-cell RNA sequencing data

Raw sequencing data from each biological sample were aligned to the human genome (hg19). The CellRanger count command was used to produce the single-cell expression data. The R package Seurat (v4.3.0) was used for subsequent gene and cell filtration, normalization, principal component analysis, variable gene finding, clustering analysis, and Uniform Manifold Approximation and Projection (UMAP) dimension reduction. Briefly, a matrix containing gene-by-cell expression data was imported to create individual Seurat objects for each sample. Cells with <200 detectable genes and >20% mitochondrial genes were excluded. Potential doublets were excluded using the DoubletFinder package, the ratio of which was determined according to Illumina's estimation (https://kb.10xgenomics.com/hc/en-us/articles/360001378811-What-is-the-maximum-number-of-cells-that-can-be-profiled-), resulting in: 2,046 fresh D3 (76.6% retention), 1,721 fresh D7 (71.3%), 2,302 cryo D3 (83.9%), and 2,243 cryo D7 cells (82.2%). Raw and analyzed data for all four datasets are available at accession number GSE233785 (part of superseries GSE233786; https://www.ncbi.nlm.nih.gov/geo/). Principal component analysis of cells identified sub-populations that were visualized using UMAP dimensional reduction into 2-dimensional clusters. Dot plots were used to present selected gene expression levels of cells for each cluster (Table S5).

Our previously published freshly-dissociated (D0) exocrine pancreas tissue dataset (accession number GSE153834) was used as the reference to perform unimodal UMAP projection.[12] Notably, this was the same donor as the fresh D3 and fresh D7 samples, but was a different donor from the cryo samples. We first created a Seurat object for our D3 and D7 scRNA-seq data as query cells. Next, we used the MapQuery() function to map our query cells to reference cells based on their gene expression profiles and used the mapped reference cell types as the basis for clustering.

Differentially expressed genes (DEGs) between fresh D0 ductal cells, suspension-cultured (including fresh and cryo) D3 ductal cells, and D7 ductal cells compared against all other non-ductal clusters were determined using the FindAllMarkers() function in Seurat. The three DEG lists were compared. Dot plots were used to present selected gene expression levels of D0 ductal cells, D3 ductal cells, and D7 ductal cells (Table S5).

Bulk mRNA-sequencing

Sequence alignment and gene counts: RNA-Seq reads were trimmed to remove sequencing adapters using Trimmomatic[70] and polyA tails using FASTP.[71] The processed reads were mapped back to the human genome (hg19) using STAR software (v. 2.6.0.a).[72] The HTSeq software (v.0.11.1)[73] was applied to generate the count matrix using default parameters.

Differential expression gene (DEG) analysis was conducted by adjusting read counts to normalized expression values using TMM normalization method in R.[74] Briefly, for between-treatment comparison, general linear models were applied to identify DEGs between 5% Matrigel (treatment) and no addition (untreated) using TMM normalization, where expression level was used as the dependent variable and treatment as the independent variable. Genes with a p-value<0.05, false discovery rate (FDR, or q-value)<0.05, and with a Log_2 fold change (FC) ≥ 1 or $\leq$-1 were considered significantly up- and down-regulated genes, respectively. In all, 568 up-regulated and 468 down-regulated genes were identified for the 5% Matrigel vs. no addition control. Raw data and DEGs are presented in Table S6 and accession number GSE233344 (part of superseries GSE233786).

Pathway analysis against HALLMARK, KEGG, and Gene Ontology-Biological Processes (GO-BP) was conducted using GSEAPreranked algorithm in GSEA Desktop program in Java.[75,76] A ranked list of whole genes by their Log_2FC was provided. Pathways with an FDR<0.05 and p-value<0.05 were considered significant. Pathways within the top 20 significant pathways are presented by their normalized enrichment score (NES); other pathways are presented in Table S6.

Electron microscopy

D7 suspension cultured cells treated with or without 5% Matrigel were diluted with 0.5 mL of wash buffer (PBS+0.3 μM $CaCl_2$). Technical replicates were pooled and washed twice using wash buffer. To maintain spheroid/cyst morphology, cells were allowed to sink by gravitational pull for at least 5 min for all washes. 1 mL of cacodylate buffer ($Na(CH_3)2AsO_2 \cdot 3H_2O$+0.3 μM $CaCl_2$, pH 7.2) was then added to cells. Once sunken, the supernatant was aspirated and 1 mL fixative solution (2% glutaraldehyde in 0.1 M cacodylate buffer) was added to cells for 5 min. The supernatant was aspirated and 1 mL fixative solution was added again to the cells for 60 min. Fixed samples were then dehydrated, embedded in Embed 812 (Electron Microscopy Sciences, Hatfield, PA), and polymerized at 64°C for 48 h. Ultrathin sections (70-nm thickness) were cut using a Leica ultramicrotome with a diamond knife, transferred to a 200-mesh EM grid, and stained with 2% uranyl acetate in 70% ethanol for 1 min followed by Reynold's lead citrate for 1 min. Electron microscopy was performed on an FEI Tecnai 12 transmission electron microscope (Thermo Fisher Scientific, Waltham, MA) equipped with a Gatan Ultrascan 2K CCD camera operated at 120 keV. Images were processed and analyzed using Adobe Photoshop.

ECM protein chip array

D1 cells were enriched for live cells using Histopaque-1077. After quantification using a hemocytometer, up to $1x10^6$ live cells in 4 mL suspension culture medium were seeded onto an ECM Select® Array Kit Ultra-36 (Advanced Biomatrix, Carlsbad, USA), which was placed inside an ultra-low attachment 6-well plate (Corning). Cells were incubated in a humidified 5% CO_2 atmosphere at 37°C with forward-back rocking at 1 rpm at a low tilt for 24 h. Cells were washed twice with room-temperature PBS and fixed using cold 4% paraformaldehyde for 15 min at room temperature. Cells were then permeabilized with PBS+0.1% Triton X-100 and stained with Hoechst 33342 (1:500; Abcam, Cambridge, UK) for 60 min at room temperature. Cells were gently washed twice with PBS+0.1% Triton X-100 and imaged on the Zeiss Axio-Cam506. Tile imaging was used to capture each individual ECM protein condition using the same exposure settings, which were adjusted for each independent experiment using the negative control to allow for quantification of the cells attached to each condition.

ImageJ version 1.8.0 was used for image analysis and quantification. Briefly, the blue channel was selected and a makeRectangle macro run to generate a uniform measurement area. Image brightness and contrast were evenly adjusted across all images and the mean gray values were measured. Mean gray values underwent Log_2 transformation, then two-tailed paired Student's t-test was used relative to the negative control (BSA) condition (Table S7). Conditions with p-value<0.05 were considered significant.

Fluorescence-activated cell sorting (FACS) for $CD133^+$ ductal cells

D1 cells were enriched for live cells using Histopaque-1077 as described above. Cell suspensions were then blocked with Human TruStain FcX (BioLegend, San Diego, USA) for 10 min at room temperature according to the manufacturer's recommendations. Biotin-conjugated anti-human CD133/2 (clone 293C3; Miltenyi Biotec, San Diego, USA) was added to cells at a 1:100 dilution and allowed to incubate on ice for 30 min. Cells were washed twice using PBS+0.1% BSA+PS+Ri then treated with 0.2 μg/mL streptavidin-labeled allophycocyanin (APC) (BioLegend) on ice for 30 min. Cells were washed twice using PBS+0.1% BSA+PS+Ri and resuspended in DAPI (0.2 μg/mL). An isotype control antibody (biotin-conjugated mouse IgG2b, clone eBMG2b; eBioscience, Santa Clara, USA) or secondary-only control was used to set gates. Cell sorting was performed on an Aria-special order research product (SORP) (Becton Dickinson, San Jose, USA). All analyses included: 1) initial gating of forward and side scatters (FSC and SSC, respectively), 2) doublet exclusion gating for high pulse-width cells (FSC-a/FSC-h and SSC-a/SSC-h), and 3) live cell gating by selecting DAPI-negative cells. The purity of sorted events was routinely >95%. Acquired flow data were analyzed using FlowJo software ver.10.8.1 (TreeStar, Ashland, USA). Returned cell populations were pelleted, resuspended in DMEM/F12+PS, counted by hemocytometer, and plated into colony assay.

QUANTIFICATION AND STATISTICAL ANALYSIS

Statistical analyses and plots were generated using GraphPad Prism 9.5 software (GraphPad Software, San Diego, USA). Colony, spheroid, and cyst diameters are expressed as truncated violin plots. All other results are expressed as mean ± SEM unless otherwise stated. Comparisons between two groups were calculated using two-tailed Student's t-test with Welch's correction, and between three or more groups using ordinary one-way ANOVA with Tukey's correction. Paired analyses were used when comparing donor means (e.g. colony-forming efficiency), unpaired analyses were used when comparing replicates (e.g. colony diameters). Results are considered statistically significant when p-value<0.05. Asterisks are used to indicate: *p<0.05, **p<0.01, ***p<0.001, and ****p<0.0001. Additional details can be found in the figure legends. At least three independent donors were used with at least two technical replicates for all experiments.